

**STOCHASTIC REACTOR MODEL FOR
SURROGATE DIESEL FUELS**

**A Thesis Submitted to
the Graduate School of Engineering and Science
of
Izmir Institute of Technology
in Partial Fulfillment of the Requirements for the Degree
of**

MASTER OF SCIENCE

in Energy Engineering

**by
Gökçen Sandal**

**December 2015
İZMİR**

We approve the thesis of **Gökçen Sandal**

Examining Committee Members:

Assist. Prof. Dr. Alvaro DIEZ
Department of Mechanical Engineering
İzmir Institute of Technology

Assist. Prof. Dr. Ünver Özkol
Department of Mechanical Engineering
İzmir Institute of Technology

Assist. Prof. Dr. Turhan Çoban
Department of Mechanical Engineering
Ege University

23 December 2015

Assist. Prof. Dr. Alvaro DIEZ
Supervisor, Department of Mechanical Engineering
İzmir Institute of Technology

Prof. Dr. Gülden GÖKÇEN AKKURT
Head of the Department of Energy
Engineering

Prof. Dr. Bilge KARAÇALI.
Dean of the Graduate School of
Engineering and Science

ACKNOWLEDGMENTS

I would like to dedicate this thesis to my family, Süleyman, Nursan, Gencay SANDAL and my beloved grandpa, who have been there for me and supported me in every decision that I have made.

I would like to express the deepest appreciation to my thesis supervisor, Dr. Alvaro DIEZ, for constant support throughout dissertation, guidance and his endless patient.

In addition, I would like to thank to Assoc. Prof. Moghtada MOBEDI, who is encouraged me since the first day in my master.

Finally, I am very grateful to my beloved friends Aygün, Burcu, Kıvanç, Elif and others for their encouragement, support, endless care and all patience during this graduate work. Thank you for expressing your belief in me any time I feel frustrated. I am really lucky to have you. I could not do it without you.

ABSTRACT

STOCHASTIC REACTOR MODEL FOR SURROGATE DIESEL FUELS

The objective of this thesis is to develop of various surrogate fuels with computational engine simulation tools based on stochastic reactor models (SRMs) in direct injection engines (DI). The SRM is based on probability density function (PDF) approach which has important ability to calculate complex reactions, energy equations and mass transfer. It is also successful to control the effects of inhomogeneities and turbulence with low computational cost.

Since the diesel fuel is very complex to solve in numerical tools, surrogate fuels were tested in this study. N-heptane, n-heptane / toluene and n-heptane / isooctane mixtures were used as surrogate fuels due to their physical and chemical properties were very close to diesel fuel. These fuels were tested under different injection timings and the calculated results were compared with an experimental study's data.

Comparison of ignition delay results demonstrate a good agreement between theoretical and experimental data, but soot formations were different when compared to literature and reference study. Fuel properties, structures or discrepancy between engine operating conditions and numerical model could be the cause of these differences.

ÖZET

DİZEL YERİNE KULLANILAN YAKITLAR İÇİN OLASILIKSAL REAKTÖR MODELİ

Bu çalışma direkt enjeksiyonlu motorlarda dizel yakıt yerine kullanılabilen, fiziksel ve kimyasal özellikleri bakımından dizel yakıtı benzer özellik gösteren çeşitli vekil yakıtların numerik olarak incelenmiştir. Hesaplamalar Olasılık Yoğunluk Fonksiyonu yaklaşımı timeline dayanarak, olasılıksal reaktör modeli kullanılarak yapılmıştır. Bu modelin en önemli avantajları homojensizliği ve türbülanslı zaman ve maliyet açısından daha kolayca ve kontrol edebilmesidir. Bu amaçla enerji ve kütle transferi denklemleri çözülmüştür.

Vekil yakıt kullanılmasının amacı, dizel yakıtın kompleks olmasıdır. Fiziksel ve kimyasal olarak dizel benzer yakıt kullanılarak zaman ve maliyetten tasarruf edilir. Bu amaçla öncelikle dizel özellikleri çok benzeyen tek zincirli bir molekül olan n-heptan kullanılmıştır. Daha sonra n-heptan / toluen, n-heptan / izooktan karışımları deneyerek, yakıt kompleksleştirilmiş ve deneysel olarak test edilen dizel ile karşılaştırılmıştır. Bunun sonucunda tutuşma gecikmeleri ve kurum miktarları saptanmıştır.

Genel olarak tutuşma gecikmesi deneysel sonuçlara benzer özellik göstermiştir. Kurum miktarı, daha önceki çalışmalara ya da deneysel sonuçlara göre beklenildiğinden farklı çıkmıştır. Yakıtların özellikleri, yapıları ya da deney koşullarının, numerik hesaplamalara göre farklılık gösterebilmesi, bu farklılığın oluşmasında bir etken olabilir.

TABLE OF CONTENTS

LIST OF FIGURES	vi
LIST OF TABLES	ix
CHAPTER 1. INTRODUCTION	13
1.1. Fuels.....	13
1.2. Computational Tools.....	14
CHAPTER 2. LITERATURE SURVEY.....	16
2.1. Surrogate Fuels	Hata! Yer işareti tanımlanmamış. 18
2.2. Numerical Studies	Hata! Yer işareti tanımlanmamış. 18
CHAPTER 3. METHODOLOGY	32
3.1. SRM	33
3.2. PDF	34
3.2.1. Operator Splitting and Numerical Solution.....	37
3.2.2. Piston Movement.....	39
3.2.3. Chemical Reactions	41
3.2.4. Heat Transfer	41
3.2.5. Heat Release Calculation.....	43
3.3. Direct Injection Models	43
3.3.1. Instantaneous Vaporisation Model	44
3.4. Surrogate Fuels	47
3.4.1. N-Heptane.....	48
3.4.2. Finding proper heat transfer coefficient	49
CHAPTER 4. RESULT AND DISCUSSION.....	50
4.1. Experimental Study.....	51
4.2. Ignition Delay Definition.....	54
4.3. Examined Fuels.....	54
CHAPTER 5. CONCLUSION	65
REFERENCES	68

LIST OF FIGURES

<u>Figure</u>	<u>Page</u>
Figure 2.1. NO _x emissions for Blend1 and Blend 2 (Puduppakkam et al. 2009).	20
Figure 2.2. Calculated UHC emissions for Blend 1 and Blend 2.	21
Figure 2.3. Ignition delay tendency of the multi-component and n-heptane surrogate models when equivalence ratio (ϕ) equals 0.5, 0.9, and 1.2.	22
Figure 2.4. Ignition delay trends of multi-component and n-heptane fuel models.	23
Figure 2.5. Ignition-delay time for the full gasoline surrogate master mechanism (solid lines) and reduced 438-species mechanism in Figure 2.4.	25
Figure 2.6. Ignition delay results for diesel and hexadecane.	27
Figure 2.7. Ignition delay results for diesel and dodecane.	28
Figure 2.8. Optical engine scheme in Aronsson study.	29
Figure 2.9. Comparison of pressure traces between optical (with three different intake temperature) and metal engines.	30
Figure 2.10. Comparison of the cylinder pressure at $\phi = 0.286$ between model predictions (lines) and experimental data.	31
Figure 3.1. Example of PDF shape for Temperature.	34
Figure 3.2. The steps in the operator splitting algorithm.	37
Figure 3.3. Piston Cylinder.	40
Figure 3.4. Geometric solution for x.	40
Figure 3.5. Operator split loop for the DI SRM including the fuel injection step.	44
Figure 3.6. When fuel m_f is added to the cylinder, the mass fractions and temperatures.	45
Figure 3.7. Schematic of an existing particle and of the ratios of masses transferred from it during fuel injection.	46
Figure 3.8. Molecule structure of n-heptane (C ₇ H ₁₆).	49
Figure 3.9. Pressure graphs for different woschni heat transfer coefficients.	50
Figure 4.1. The Optical chamber in experiments.	52
Figure 4.2. Ignition delays for experimental diesel results related to cylinder pressure.	53
Figure 4.3. Ignition delays for experimental diesel results related to luminosity.	53
Figure 4.4. Start of Injection N-Heptane value (SOI 35° BTDC).	56
Figure 4.5. Determination of the start of combustion n-heptane (SOC 35° BTDC).	57
Figure 4.6. Experimental and numerical comparisons of n-heptane.	58

Figure 4.7. Ignition delays comparisons regard to the experimental diesel from pres ...	60
Figure 4.8. Ignition delays comparisons regard to the experimental diesel from luminosity	61
Figure 4.9. Differences between experimental and numerical pressure.	62
Figure 4.10. Soot comparison for different injection timings for n-heptane.	63
Figure 4.11. C ₂ H ₂ results versus crank shaft for tested fuels (SOI 10° BTDC).	64
Figure 4.12. C ₂ H ₂ results versus crank shaft for tested fuels (SOI 35° BTDC).	65

LIST OF TABLES

<u>Table</u>	<u>Page</u>
Table 2.1 Current surrogate fuel blends (Puduppakkam et al. 2009)	17
Table 2.2 Properties for average gasoline and diesel in the USA (Naik et al. 2010).	23
Table 3.1. Typical Diesel fuel composition.....	47
Table 3.2 Properties of diesel, n-heptane & IDEA fuel.....	48
Table 3.3 Properties of diesel, n-heptane, toluene fuel.....	48
Table 4.1 The Engine specifications.....	52
Table 4.2 Ignition delays for surrogate fuels.	59
Table 4.3 Properties of the fuels at standard atmospheric conditions.	64

LIST OF SYMBOLS

Symbols

A	Area	m^2
B	Bore	m
C	Heat Capacity	J/K
c_p	Specific heat at Constant Pressure	J /kg K
F/A	Fuel-air Ratio	-
M	Molar Mass	kg /kmole
N	Crankshaft rotational Speed	rev/s
E	Energy	J
Q_{loss}	Heat loss	J
D_h	Hydraulic Diameter	m
h_g	Heat Transfer Coefficient	W/m^2K
H	Enthalpy	J
U	Heat Transfer	J
ψ		kmole/ s
R	Universal gas constant	J/K mol
h	Specific Enthalpy	J/kg
F	The MDF	-
m	Mass	kg
p	Pressure	Pa
t	Time	s
T	Temperature	K
ω	Global Reaction Rate	kmole/ m^3s
λ	Air-fuel Equivalence Ratio	
X	Mole Fraction	-
Y	Mass Fraction	-
φ	Vector of Random Variables	-
ρ	Density	kg/m^3
W	Work	J
η	Efficiency of Engine	

γ	Specific Heat Ratio	-
Q_i	Source/ sink Term for The Variable i	
θ	Crank angle	degree
ψ	Realisation (sample space) Variable	
V	Cylinder Volume	m^3

Abbreviations

<i>DI</i>	Direct Injection (compression ignition)
<i>CFD</i>	Computational Fluid Dynamics
<i>RPM</i>	Revolutions Per Minute
<i>rc</i>	Compression Ratio
<i>CAD</i>	Crank Angle Degree
<i>HRR</i>	Heat Release Rate
<i>HCCI</i>	Homogeneous Charge Compression Ignition
<i>EGR</i>	Exhaust Gas Recirculation
<i>MDF</i>	Mass Density Function
<i>MPI</i>	Message Passing Interface
<i>TDC</i>	Top Dead Center
<i>BDC</i>	Bottom Dead Center
<i>SOI</i>	Start of Injection
<i>SOC</i>	Start of Combustion
<i>MFB</i>	Mass Fraction Burned
<i>SI</i>	Spark Ignition
<i>SRM</i>	Stochastic Reactor Model
<i>PSFC</i>	Power specific Fuel Consumption
<i>PaPFR</i>	Partially Stirred Plug Flow Reactor
<i>PDF</i>	Probability Density Function

Subscripts

<i>ad</i>	Adiabatic
<i>b</i>	Burned Gas
<i>cyl</i>	Cylinder
<i>Ma</i>	Mach Number
<i>inj</i>	Injection
<i>f</i>	Flame

<i>r</i>	Chemical Reactions
<i>u</i>	Unburned
<i>amb</i>	Ambient Conditions
<i>fg</i>	Fresh gas Conditions
<i>w</i>	Wall
<i>m</i>	Mixing Mass
<i>vap</i>	Vapour
<i>I</i>	Species

CHAPTER 1

INTRODUCTION

Rapid growth of the world population, and industrialization cause more energy needs. Combustion engine is one of the major sources for energy production although it has negative consequences. The usage of combustion process leads to the problem of emission, since main combustion sources are fossil fuels. Emissions result in pollution, poisoning and global warming. The limited fossil fuels sources, polluting and economical problems are encouraged companies and researchers to change and develop engine-fuel technology more in order to provide reduction in environmental inquination.

1.1. Fuels

Diesel is a mixture of hydrocarbons obtained by distillation of crude oil. The important properties in order to characterize diesel fuel include cetane number fuel volatility, density, viscosity, cold behavior, and sulfur content. Diesel fuel specifications differ for various fuel grades and in different countries. Development of alternative diesel fuels, once promoted by the desire to reduce exhaust emissions, is now increasingly being driven by climate change issues and energy security. The most important alternative fuel option includes synthetic fuels, biodiesel, dimethyl ether, alcohols, methane, and hydrogen. However, petroleum derived fuel is the main source for automotive engines.

Measuring the exact fluid composition of each diesel fuel batch, delivered from refineries, is very difficult, since crude oil diesel fuels consist of hundreds of chemical components. Chemical reactions typically do not show a linear dependence on all the variables composition, temperature and pressure. Understanding chemical reduction processes and using realistic diesel fuels in numerical simulations are very complicated. For this reason, surrogate fuels approach has been developed.

Surrogate fuels are simpler versions of fully blended fuels. They comprise of particular species with known concentrations and similar combustion characteristics to the real fuel. Since the surrogate fuel components are not complex as real fuel, finding fluid properties and, chemical reaction mechanisms become less time consuming. Experiments with surrogate fuels are useful, since the chemical and/or physical complexity of the fuel can be limited and vaporization, mixing, ignition, and primary pollutant formation processes are easier to understand. Usually surrogate studies involve more than one component. The chemical, physical structure and molecular weights of surrogate fuels have to be similar with diesel fuel components characteristics. In order to create accurate model according to the experimental data, a validated, detailed chemical kinetic models of the multicomponent surrogate mixture have to be developed. The ultimate aim is to translate these findings back into design rules of the real fuel/engine combination.

1.2. Computational Tools

Since the alternative fuels are expensive or unpractical, energy production through combustion of fossil fuels will probably continue to be the major source for many decades. Since the combustion of fossil fuels will have important role for many years, strong efforts need to be made in order to achieve more efficient ways for energy production and energy usage. Therefore, experimental studies are supported with numerical studies.

In the classical engine testing methods, experiments are done under laboratory conditions. Nevertheless, constructing an experimental set up is not cost ineffective and it is time consuming, since obtaining necessary outputs/results from the experimental set up is required to change constantly. Therefore, numerical study will procure better insight of the parameters than experiments with regard to money and time. The new approach of engine design shows a close interaction between numerical and experimental studies. Therefore, new numerical methods are developed to understand the diesel engines emissions and productivity.

An efficient computational tools comprise the molecular transport, turbulent flow and chemical kinetics in order to design high efficiency and low emission engines

and these enhanced models have to be practical for users to perform fast and easy numerical simulations to predict all possible operating conditions of an engine. However, still significant uncertainties exist in these fundamental processes and their usage in reality.

CHEMKIN and Computational Fluid Dynamics (CFD) tools are the most known simulation programs. However; another commercial program, LOGEsoft, is used in this study as an alternative to these programs, which is cost and time effective. In this study, engine performance is reviewed by testing alternative surrogate fuels. Conducted numerical study is evaluated for findings by comparing experimental studies.

Reduced chemical kinetic models could be developed in order to be used in LOGEsoft calculations. The tool is derived from detailed chemical kinetic mechanisms, which are also validated according to mathematical principles. In order to resolve the chemistry in reacting flows, LOGEsoft requires long computational time, which is directly affected by two factors. The first one is due to large number of species and reactions, and the second is the computational hardness due to the extensive range of timescales, which are presented in chemically reacting systems. Mechanism reduction can be formed by eliminating insignificant species and reactions (those reactions and species do not affect the main target, particularly) which is also called skeletal reduction.

Stochastic reactor model (SRMs) is available in LOGEsoft panel and could be applied for different engine types such as spark ignition engine (SI), homogenous charge compression ignition engine (HCCI) and direct injection engine (DI). The SRMs has a balance between detailed calculations for engine emissions and performance. It provides useful predictions for the combustion processes in an engine with high level of details, accuracy, speed and easiness to use.

The presented work is about developing a realistic combustion computational methodology according to experimental database with reference fuels, which are representative actual commercial diesel fuels.

The aim of this study is to identify suitable mixture for diesel engines by comparing the numerical outputs with the experiments. In this study, LOGEsoft commercial computational software is used and engine performance is reviewed by testing the alternative surrogate fuels. Their physical properties are in line with the commercial diesel fuels. Numerical study is evaluated for findings by comparing

experimental study. The reactor type of SRMs is used in DI engines while fuels were chosen to be n-heptane and n-heptane/toluene mixture and primary reference fuels (PRF) are used. The numerical simulation method is based on Probability Density Function (PDF). In the search of a proper fuel mixture for diesel engines, the results for these indications are presented.

Since the work relates to the simulation of engines, surrogate fuels and stochastic reactor model, an account of the basic principles of these are provided in Chapter 2 which is based on literature.

Chapter 3 is an overview of methodology. It also demonstrates common techniques that are used to simplify chemical models to make them practical for use in engine simulations. The theory behind the Stochastic Reactor Models which is Probability density function (PDF), and their practical implementation are described in this part.

In Chapter 4, the results are presented and described in details. In the last chapter presents conclusions of this work.

CHAPTER 2

LITERATURE SURVEY

Fossil included in hydrocarbon fuels are the primary energy resources in the world. Approximately, 60% of fossil fuels are used in transport sector. Since fossil fuels include high amount of green house gasses (GHG), they are widely responsible for the emission of a significant amount of pollutants in the atmosphere. The current climate changes and fuel prices lead to improvement in the performance of engines. In order to have better engine performance and reduce pollutant emissions, scientific studies are in progress. For this reason, chemical kinetics will be essential to design better performance engines with lower emissions (Pepiot 2008) (Seidel et al., n.d.)

In order to improve combustion efficiency, engine design and to reduce the formation of pollutants, fuel oxidation chemistry should be understood in detail. Therefore, numerical studies are made to accelerate the studies about development alternative methods in addition to the experimental studies.

Nowadays, petroleum-derived fuels constitute a large portion of our energy resources and involve hundreds of different chemical compounds. Since the chemical reactions show non-linear dependence on the variables temperature, pressure and composition, using real fuels for numerical simulations are difficult. For the reason of the difficulties about detailed chemical modeling of real hydrocarbon fuels (diesel and gasoline fuels are defined as real fuel), fuel representation is used in numerical simulations of combustion engines. As a consequence, surrogate fuels are adapted by the scientific world. They are simpler representations of fully blended fuels. Using surrogate fuels instead of real fuels represents numerous advantages such as reproducibility and possibility of formulating suitable chemical models for computational tools (Pepiot 2008) (Seidel et al., n.d.).

2.1. Surrogate Fuels

Since the chemical and physical properties are similar, surrogate fuels are identical to the actual fuel. Surrogate fuels are comprised of selected species of known concentrations and they exhibit combustion characteristics similar to those of the real fuel. Even though, a surrogate fuel does not need to contain same components with a diesel fuel to show the real fuel behavior, similarities are important to let better agreement. Usually simplified alkanes with equivalent carbon number with real fuel are used as a surrogate fuel. They are typically adopted in order to simplify the chemistry (Smallbone et al. 2010). Therefore, the researchers have focused to define a suitable set of surrogates for different types of fuels. For surrogate fuel approach, different targets such as properties, developments and application targets are considered (Farrell, Cernansky, and Dryer 2007) (Krishnasamy et al. 2013).

2.2. Numerical Studies

Recent improvements in chemical kinetics have brought more valid fuel models capable of computing the combustion characteristics of the higher molecular weight hydrocarbon fuels. Today, complexity of engine design is a growing situation. Thereby, the companies endeavour to maintain a high level of engine performance while using a wider variety of fuels with continuing to reduce emissions. Therefore, simulation tools replace with conventional engine experiments for engine design and engine development and they become a need for automotive engineers. In addition to the many effects of engine combustion modeling, modeling of the fuel chemistry is important to solve the complexity associated with fuel effects. For example, parameters such as soot formation in diesel engines correlated with fuel structures besides engine operating conditions (Liang et al. 2010). In order to have more predictive combustion results, realistic combustion chemical kinetics should be applied. For this reason, researchers try to improve the use of simulation tools to reduce mechanisms and develop better engine efficiency. CFD, Chemkin packages can be given as examples for popular simulation tools.

Some studies about surrogate fuels and their application methods by numerically make a contribution for this study.

Pitz and Mueller have developed chemical kinetic models for n-alkenes up to 16 carbons. They worked with experimental studies about surrogate fuels for chemical modelling. Lower molecular weight surrogate components such as n-decane and n-dodecane, which are the most relevant to jet fuel surrogates, were used. The two ring compounds such as decalin and tetralin were tested as fuel by them. They also published kinetic mechanisms for compounds of lower molecular weights with similar typical biodiesel for esters. Multi-component surrogate fuel mixtures were studied to compare the results with real diesel fuel. The mechanism reduction tools were tried as practicable model, because of the detail chemical mechanisms of surrogate fuels in significant large size. The purpose of the paper is to remain the major research gaps. In this study, for the chemical classes of esters and cycloalkanes, experiments and modeling on higher molecular weight components are attempted (Pitz and Mueller 2011).

In order to have an accurate prediction of combustion phase and emissions, model-fuel blending methodology suits to simulation of fuel specific characteristics such as fuel vaporization, emissions or ignition timing. Puduppakkam et al. presented a surrogate blending technique and they used a practical modeling tool in order to determine proper surrogate blends. The surrogate blends were tailored to different fuel characterization for engine simulations. They chose a range of potential model fuel components based on the characteristic chemical classes present in real fuels. In order to predict combustion phasing and emissions due to validation of surrogate-blending methodology, CHEMKIN-PRO, multi-zone engine model was used. Three surrogate fuel blends were simulated and ignition timing, NO_x, heat release and unburnt hydrocarbon emissions results were compared with engine data.

Table 2.1 Current surrogate fuel blends (Puduppakkam et al. 2009)

Fuel	% Composition by weight				
	iso-octane	n-heptane	Toluene	methyl cyclohexane	1-hexene
Blend 1: 5 component	51	14	25	5	5
Blend 2: 4 component	29	13	29	29	0
Blend 3: PRF 91	91	9	0	0	0

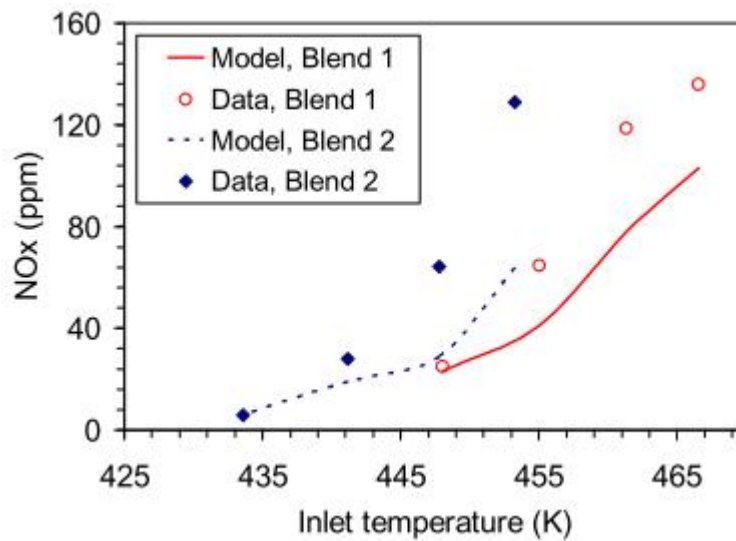


Figure 2.1 NO_x emissions for Blend 1 and Blend 2 (Source: Puduppakkam et al. 2009).

Generally, NO_x is mainly formed in the load hot zones, and it increases with inlet temperature. Thus, thermal NO_x would be expected to be higher. In this study, the engine data and the model predictions showed this trend for all the fuels. All calculated values, and trends with inlet temperature, were consistent with the engine data. Engine data showed that the NO_x values for the market gasoline were significantly lower than for fuel blends 1, 2 and 3.

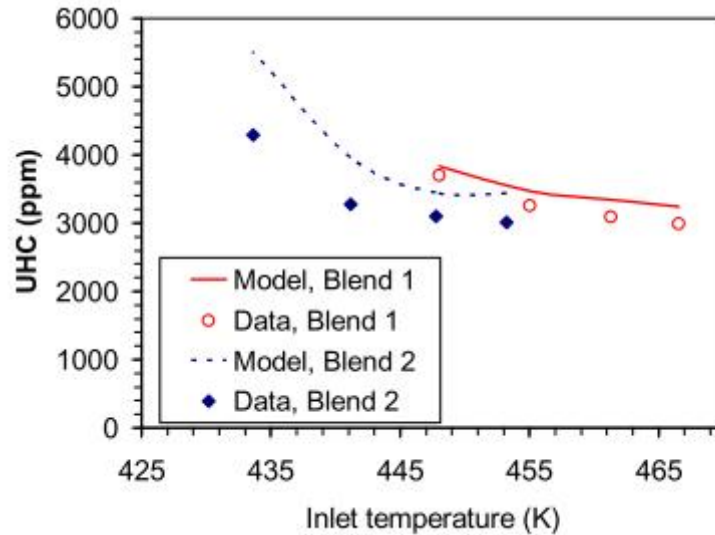


Figure 2.2 Calculated UHC emissions for Blend 1 and Blend 2 (Puduppakkam et al. 2009).

The unburnt hydrocarbons are mainly formed in the crevice zones when combustion occurs close to TDC. With decreasing of inlet temperature, the unburnt hydrocarbon concentration increases.

Puduppakkam et al. detected that the surrogate fuel blending methodology with multizone engine combustion are efficient and effective to investigate HCCI gasoline combustion. The multizone model was applied with KIVA-3V. Their results matched the correct trends for combustion phasing, and the emissions of NO_x and UHC and using the multi-zone model saved a reasonable amount of time (Puduppakkam et al. 2009).

X. Su et al. studied a novel methodology for surrogate models which based on a local optimization and sensitivity analysis technologies. In the proposed approach, several important fuel properties were considered. Under the physical properties, they focused on volatility, density, lower heating value (LHV) and viscosity, while the chemical properties related to the chemical composition, hydrogen to carbon (H/C) ratio and ignition behavior. The volatility is important for evaporation, emission and combustion efficiency. Density effects the injection shape, lower heating value is important for total energy release.

The tested surrogate fuels were simulated in a multi-dimensional engine under low temperature combustion (LTC) against the known experimental data. They also compared the results with a single component model. In single component model, n-

heptane represented for chemical property, n-tetradecane represented for physical property.

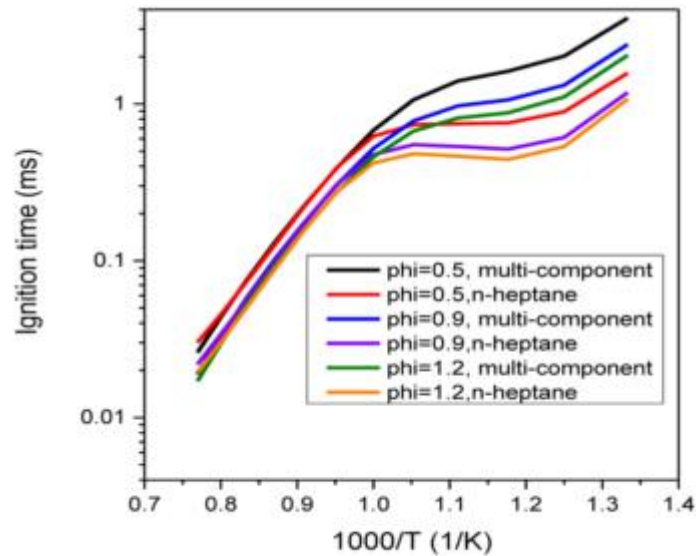


Figure 2.3 Ignition delay tendency of the multi-component and n-heptane surrogate models when equivalence ratio (ϕ) equals 0.5, 0.9, and 1.2 (Source: Su, Ra, and Reitz 2014).

The results were compared in Figure 2.3. They showed that in the high temperature regime, there were no differences in the ignition delay values between the different fuel models. However, at temperature regimes relevant to fuel ignition in actual engine conditions, the ignition delay for the n-heptane model was significantly lower than that for the multi-component fuel model (equivalence ratio (ϕ) equals 0.5, 0.9, and 1.2). Since the cetane number of n-heptane (CN=56) is larger than the cetane number of the multi-component fuel model (CN=47.9), this trend agrees with the actuality.

The proposed surrogate fuel model predicted the overall emissions and combustion process, however the single component model was unable to predict the combustion process and emissions for the low cetane diesel fuel in the LTC condition (Su, Ra, and Reitz 2014).

Krishnasamy et al. tried to develop surrogate models which can be applied to predict conventional and low temperature combustion (LTC) characteristics of the three fuels in a single cylinder diesel engine. In order to do the simulations, the KIVA-ERC-CHEMKIN code was used and it incorporated with MultiChem mechanism. In this mechanism 120 species and 459 reactions were qualified. The results were compared

with the measured experimental data. The fuels cetane numbers range was approximately 40-57. To understand the advantages of using the multi-component models, the results were compared with a conventional single component model. N-tetradecane physical properties and n-heptane chemistry were taken as reference (Krishnasamy et al. 2013).

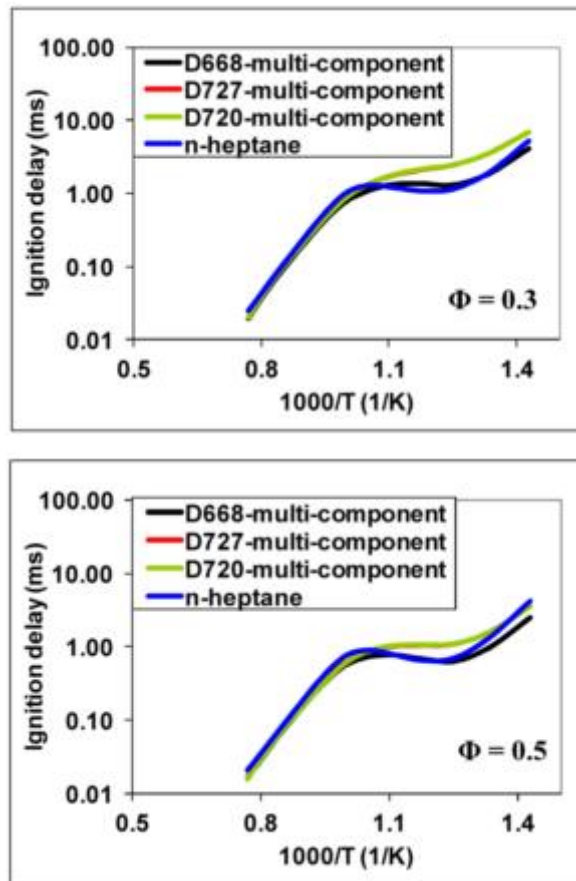


Figure 2.4 Ignition delay trends of multi-component and n-heptane fuel models (Source: Krishnasamy et al. 2013)

A comparison of the performance of the present a single component surrogate models with conventional multi component model showed that it was unable to predict combustion and emission processes in LTC operation was the diesel fuel has low cetane number. The engine trends showed much higher sensitivity to fuel type under LTC conditions, whereas the sensitivity was very specific in conventional combustion (Krishnasamy et al. 2013).

Naik et al. developed a software tool in order to use detailed chemistry in representing conventional fuels in CFD simulation. CHEMKIN-PRO was used as software tool. They started with a detailed reaction mechanism for a fuel which contains

chemistry over 3800 species and 15000 reactions including. A methodology for systematically generating surrogate blends for conventional fuels. Real fuels chemical compositions are listed in Table 2.2 and they generated the surrogate for a typical diesel in the U.S, which captures the combustion and emission characteristics of U.S. diesel.

Table 2.2 Properties for average gasoline and diesel in the USA (Naik et al. 2010).

Hydrocarbon Class (liq. vol %)	Gasoline	Diesel
<i>n-, iso</i> -paraffins	33-79	25-50
Olefins	1-18	0-2
Aromatics	10-45	15-40
Naphthenes	2-10	15-60
Molar H/C ratio	1.72-2.03	1.8
Octane or Cetane number	90-100 (81-88)	40-56
LHV (MJ/kg)	42.5-44.8	43
Molecular weight (g/mol)	98.9-105	222
Density (g/cc)	0.738	0.82-0.86
T50 (K)	368	548
Carbon number range	5-8 (4-12)	10-17 (9-24)
Avg. formula	C _{7.3} H _{14.8}	Varies

One of the aim of this work was to develop an automated way to optimize the complex surrogate blend to closely match the properties of a real fuel and to develop available, accurate and validated surrogate fuel mechanism.

The master mechanism can be reduced for the surrogate blend so that it can reproduce selected targets, such as ignition times, laminar flame speeds, fuel and emission concentration profiles, or any other properties from the available model in the tool. They presented an application to define a composition for an eight-component surrogate for a typical gasoline in the U.S. that captured most characteristics of a real gasoline. Composition for a four-component surrogate for a typical diesel in the U.S. was also generated, which captures the combustion and emission characteristics of U.S. diesel. The gasoline surrogate had 1833 species while diesel surrogates consisted of 3809 species in detailed reaction mechanism.

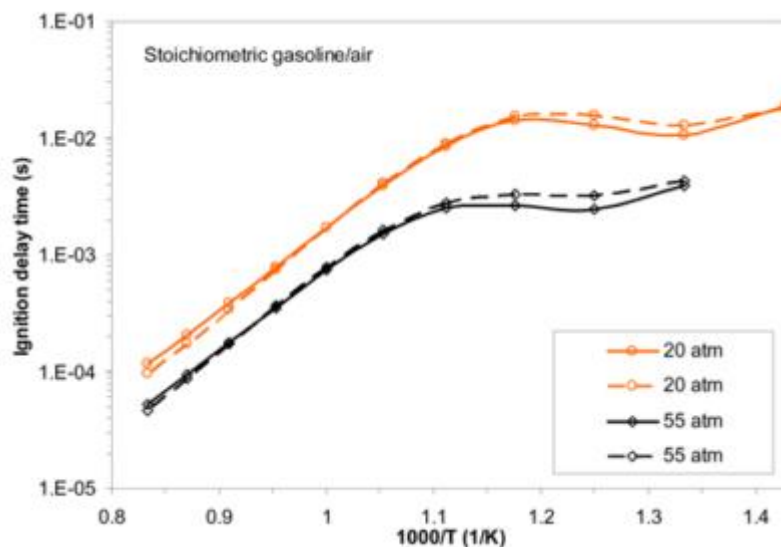


Figure 2.5 Ignition-delay time for the full gasoline surrogate master mechanism (solid lines) and reduced 438-species mechanism in Figure 2.4 (Source: Naik et al. 2010).

Figure 2.5 shows the comparisons of the predictions over the entire range of conditions considered. The results show that the reduced mechanisms perform very well when compared to the master mechanisms, since the results closely match with master mechanism. These master mechanisms for surrogates have been reduced by using several different reduction methods, testing the accuracy and efficiency of different strategies. A combination of methods resulted in a 438- species gasoline surrogate mechanism and a 436-species diesel surrogate mechanism. The reduced mechanisms are accurate for using in engine modeling and able to predict chemical speciation during engine combustion (Naik et al. 2010).

The influence of the addition of oxygenated hydrocarbons to diesel fuels has been studied by Curran et al. (2001) Detailed chemical kinetic mechanism was used in the study. N-heptane was chosen as surrogate fuel and methanol, ethanol, dimethyl ether, dimethoxymethane and methyl butanoate were used as oxygenated fuels. How soot precursors were affected by using oxygenated fuels was examined. In order to reduce emissions for diesel engines in vehicles, oxygen was added to the fuel. Generally, an oxygenated compound is added to normal diesel. Miyamoto et al. showed experimentally that addition of oxygenates to automotive fuel reduces CO and hydrocarbon emissions. This study showed oxygenated fuel effects on emissions by analogically. The results have shown that when the overall oxygen content in the fuel

reached approximately 30-40 % by mass, production of soot precursors fell effectively to zero. (Curran et al. 2001).

Çalık et.al studied to reduce emission in diesel engines by using computational fluid dynamics. NO_x-soot tradeoff is the main emission problem for diesel combustion and this problem is not eliminated with the in-cylinder combustion techniques. The aim of the study was mainly to investigate the formation and reduction of soot and NO_x emissions in diesel engine. The study was performed in Heavy Duty Diesel (HDD) engines with the help of CFD engine modeling, CHEMKIN-II and KIVA- 3VR2 package. Chalmers' Diesel Oil Surrogate (DOS) model was used which comprised of a blend of aliphatic and aromatic components. N-heptane (70%) was used as aliphatic and toluene (30%) was used as aromatic. DOS and detailed chemical reaction mechanism were formalized when comparing the ignition delay (ID) with the existing shock tube data for different temperatures at different pressure. However, present reaction mechanism was modified in order to improve its NO_x-soot emissions behavior, which was still weak. Different fuel injection times, loads and both EGR cases were studied to widen the modeling capability. Different injection timings were tried (-5, 0, 5) in the Volvo D12C DI diesel engine.

Rate of Heat Release (RoHR) increased maximum rate when related to the results. The reason of this increment was premixed combustion phase, which caused an increase in ID times. The ignition occurred after the completion of fuel injection process similar with the HCCI combustion mode. All cases, which were tried in this study, had accurate results (calculation results for in-cylinder pressure, temperature, RoHR and combustion efficiency). When they were compared to experimental results, the emissions of NO_x and soot were well. Although tendency of the calculated emissions is good, a quantitative improvement for emission predictions, especially for soot emissions, is required. Hence modeling of soot emissions is very hard. NO_x formation is also strictly coupled with the soot-oxidation process because of the remained oxygen radical. Oxygen radical is necessary for NO formation depends on the soot oxidation process. If soot-oxidation part is dominant in the mechanism, then excessive soot oxidation process can cause lower soot emissions than the real amount by consuming most of the available oxygen radical which will be used later for the NO formation reactions. In conclusion, excessive soot oxidation gives less soot emissions and prevents proper amount of NO formation indirectly (Çalık, Ergeneman, and Golovitchev 2009).

In their study Diez et al. aimed to develop a validation tool for diesel surrogate. Hexadecane and n-dodecane were used as surrogate fuels and their numerical and experimental results were compared in the study.

For experimental study, optical combustion chamber was used and the results were compared with stochastic reactor engine models. The DI-SRM model was used to find auto-ignition of n-dodecane and it was compared with the experimental data. OH initiation leading to determine ignition delay showed accurate agreement with the ignition delay from the luminosity experiments. The results showed that the minimum ignition delay belongs to hexadecane.

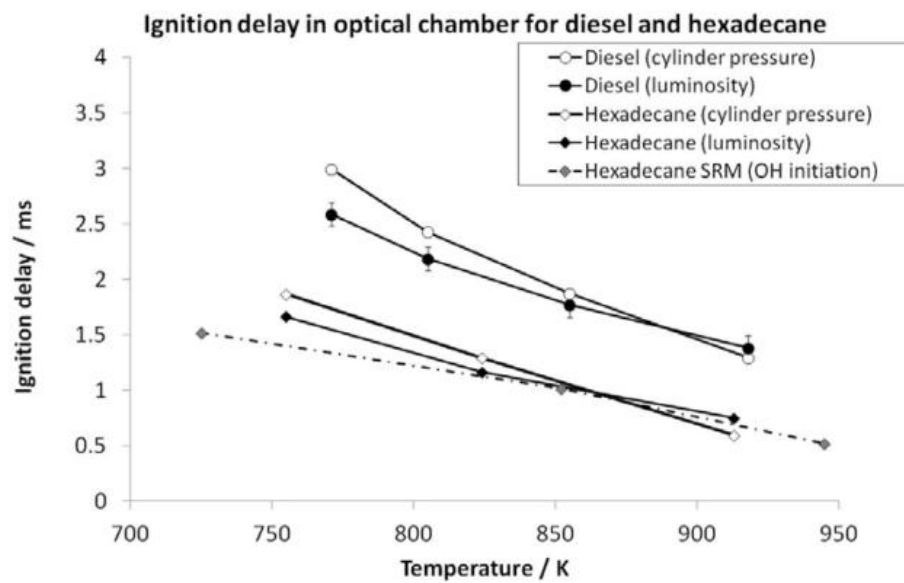


Figure 2.6 Ignition delay results for diesel and hexadecane (Diez, Løvås, and Crookes 2000)

Pressure traces for dodecane was more similar to diesel in terms of premixed and mixing controlled phases differing only on ignition delay.

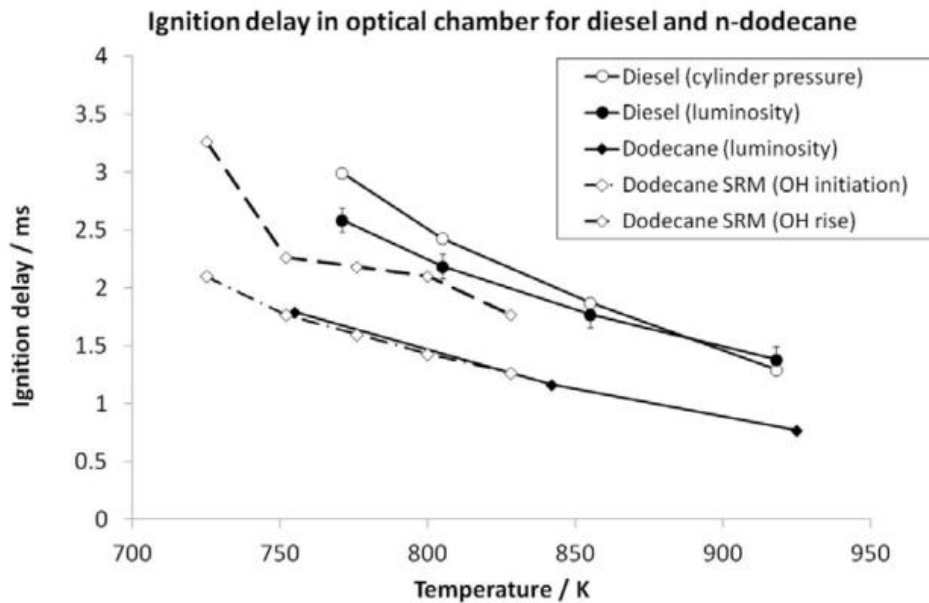


Figure 2.7 Ignition delay results for diesel and dodecane (Diez, Løvås, and Crookes 2000)

At lower temperatures the ignition delay predicted by the model was shorter than calculated experimentally, which could be caused by the assumption that the fuel is fully evaporated at the time of injection (Diez, Løvås, and Crookes 2000).

In his thesis, Bjerkborn developed a flame propagation with zero dimensional engine simulation tool which is called DARS 0-D SRM. Creating a model, which can be replaced or complemented with the Wibe function, was the purpose of this study. Also, Bjerkborn tried to avoid curve fitting when certain parameters were changed and had predictive capabilities. Monte Carlo model was created for this purpose and good correlation was found between experimental and numerical results in this study. Comprehensive informations about DARS 0-D SRM tool in this study was a guide for my study.

Aronsson et al. studied on optical engines. The purpose of the research was to investigate how the optical access affected the combustion process. They tested different loads, injection timings, injection pressures and inlet temperatures. They found that the wall heat losses in optical engines were lower than in all metal engines due to the lower heat conductivity of optical parts. Furthermore, optical engines often had larger crevice volumes due to a lower piston of the piston rings. They aimed to analyze how these differences affected the heat release and emission in optical engines.

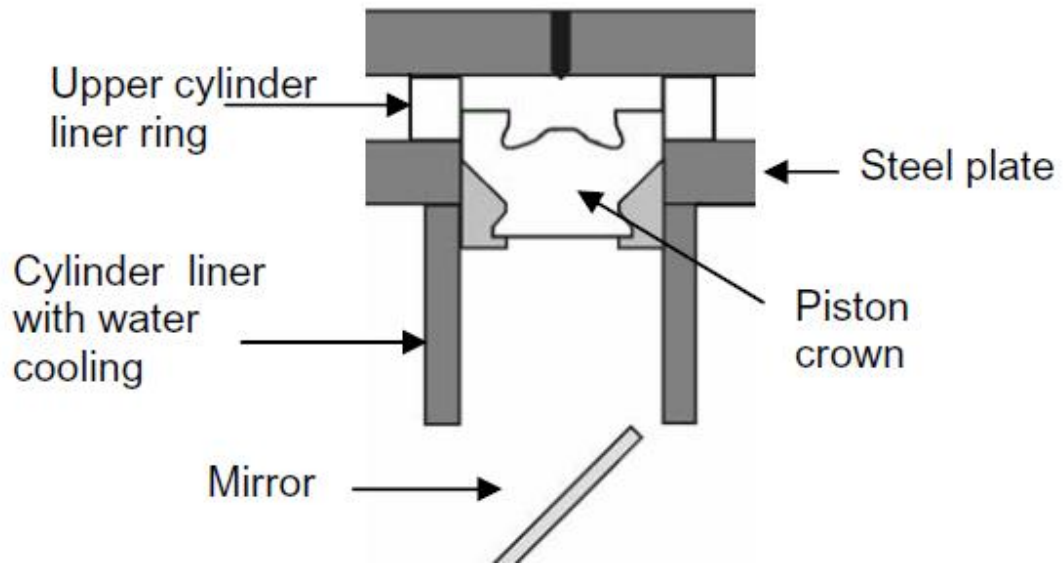


Figure 2.8 Optical engine sheme in Aronsson study (Aronsson et al. 2008).

Their heat transfer model was taken as reference for the present study since it was based on woschni heat transfer model. The heat transfer coefficients were tuned for optical engine specifications respect to the heat release curves regarding to the experiments (Aronsson et al. 2008).

The metal and optical single cylinder diesel engines were compared with the same nominal geometry at low temperature combustion conditions (Colban et al. 2008). Engine out emissions and cylinder pressure were compared with optical and metal engines and it was found that optical engine pressure and heat release characteristics were influenced by the larger crevice volumes and compliance of the extended optical piston.

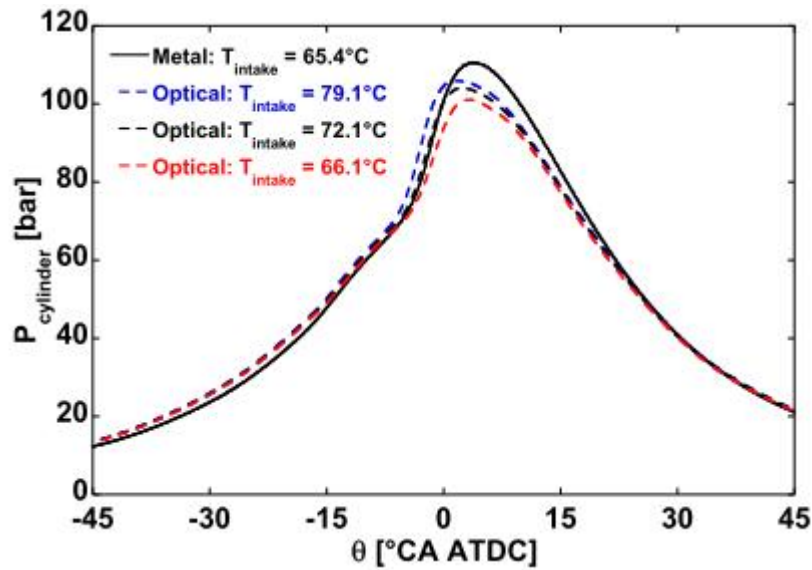


Figure 2.9 Comparison of pressure traces between optical (with three different intake temperature) and metal engines (Colban et al. 2008).

The results showed that even though combustion phasing and load were matched, the peak pressure in optical the engine was lower than metal engine. Since they assumed that premixed combustion event was constant volume process, this approximation was reasonable regarding to piston motion which was minimal during from -7.5°CA to the time of peak pressure. (The max. displacement was taken as 0.35mm in the study.) (Colban et al. 2008).

Ahmet et al. studied reduction mechanisms for fuel mixtures. Despite the fact that detailed chemical reaction mechanisms provide more information about the ways to improve modeling tools or fuel qualities in combustion process, using chemical reaction mechanisms with a complex reactor model in simulations are limited by the large number of species.

Ahmed et al. presented a chemistry guided reduction (CGR) approach which is based on chemical lumping and species removal (Ahmed, Mauss, and Zeuch 2009). N-heptane were derived a skeletal model by CGR in Ahmet et al. study. The mechanism consisted of 110 species, 1174 forward and backward reactions. Also, the mechanism was validated against the full range combustion conditions. These conditions were low and high temperatures, pressures between 1 bar and 40 bar, local and global parameters.

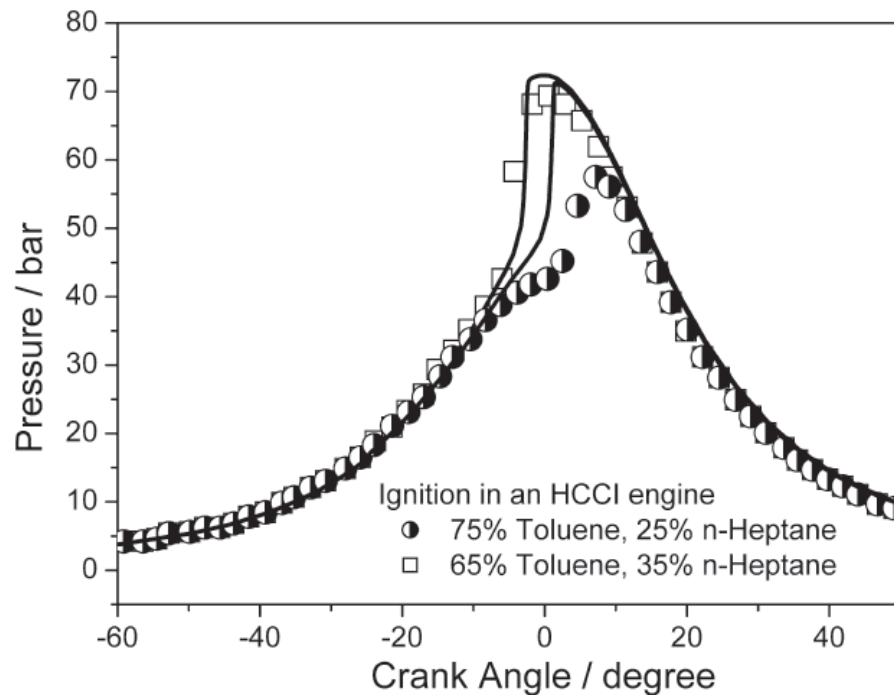


Figure 2.10 Comparison of the cylinder pressure at $\phi = 0.286$ between model predictions (lines) and experimental data.

According to the results, the larger n-heptane fraction had a good agreement for the timing. However the pressure increase prior to autoignition is overestimated for the fuel with larger toluene fraction, the autoignition and higher toluene fraction was still captured by the model (Ahmed, Mauss, and Zeuch 2009).

In the chemical lumping, species with the similar composition and functionalities are lumped into one representative species (Pepiot-Desjardins and Pitsch 2008). In the each lumping group, statistical information on the distribution of the isomers was gathered by using simulations. These distributions are stated as functions of time and space. The distribution functions approximated as the conditional averages depending on the independent state space variables. When this approach is simplified further, the resulting chemical mechanisms are used directly in chemistry packages, according which the isomer distributions depend on temperature, and the correcting factors are integrated with the Arrhenius form of the rate coefficient of lumping reactions. In this paper, authors studied the effects of lumping procedure on sensitivities of the kinetic mechanisms. For this purpose, they used n-heptane and isooctane. The results showed a good agreement between the predictions obtained using lumped and detailed mechanisms (Pepiot-Desjardins and Pitsch 2008).

A new model for the numerical simulation in the HCCI engine was presented by Kraft (2000). The model was the partially stirred plug flow reactor (PaSPFR) which is efficient to simulating inhomogeneities in the cylinder. These inhomogeneities occurred by the thermal boundary layer adjacent to the cylinder surface and caused to carbon monoxide (CO) and hydrocarbon (HC) emissions.

In this study, SRM was used to model the influence of the cold air/fuel mixture, CO, HCs in the HCCI engine. Boundary layers' and crevices' structure were modeled according to the heat and mass transfer principles. At the end of the study, unburned HCs and CO were measured in the exhaust. They compared the model's results with an experimental study which was performed compressed plug flow reactor (cPFR) (Kraft et al. 2000).

CHAPTER 3

METHODOLOGY

In the present study, zero dimensional (0-D) stochastic reactor model (SRM) is used to examine effects of various surrogate fuel effects in direct injection engines (DI) by using LOGEsoft. The principle of the SRM is based on the probability density function (PDF) approach. The most important ability of the SRM is that the program controls the effects of in-homogeneities and turbulence with low computational cost. Stochastic reactor models (SRMs) are applied to find the results for surrogate fuels in this study. LOGEsoft, which is a commercial package simulation model allows for homogenous charge compression ignition engine (HCCI) modeling, spark ignition (SI) modeling, and direct injection (DI) engines (Barkhudarov et al. 2011).

3.1. SRM

Containing the means to define the variations within the cylinder while employing detailed chemistry, micro mixing and heat transfer, exhaust gas energy and the combustion process can be studied with SRM. The SRM is employed in zonal models where kinetics has been used to predict knock and self ignition, and it is used to predict the mixing and kinetics which control the combustion processes, alongside pollutant emissions in DI engines. The strength of the SRM provides means to include the effects of inhomogeneities and turbulence. The SRM is based on the assumption of homogeneity within the combustion chamber. It is replaced by the one of statistical homogeneity, with physical quantities described by PDF distributions. Generally, homogeneous reactor model (HRM) and SRM can be used for simulations if large chemical models are employed. Also, these models can be used if transient effects need to be studied. Zero dimensional (0-D), one dimensional (1-D), two dimensional (2-D), three dimensional (3-D) modeling can be calculated by both HRM and SRM. In the 0-D, there is no spatial information to be gained from calculations of the combustion

within the cylinder. The SRM is known as a quasi 0-D tool where the spatial description is replaced with a statistical description of the distributions.

3.2. PDF

The probability density function approach is a suitable method for turbulent-reactive flows due to complex reactions which can be treated without modeling assumptions. The fluid within the solution domain is represented by a large number of computational particles in the PDF method. Each particle in the composition evolves a set of ordinary differential equations.

In the PDF method, the mass within the cylinder is divided into an arbitrary number of virtual packages called particles. Each of these particles has a chemical composition, a temperature and a mass. The particles can mix with other particles and exchange heat with the cylinder walls. Although the SRM model can be defined with a dimension in any CFD model, which requires spatial distributions of the particles with boundary condition as in the case of real engines, SRM model is chosen as 0-D in this study, which does not require any information regarding the position of the particles. LOGEsoft software reaches the solution by using PDF. It calculates the chemical composition, temperature and mass distributions of the fuel injected to the computational domain with random variable (Saxena and Pope 1999).

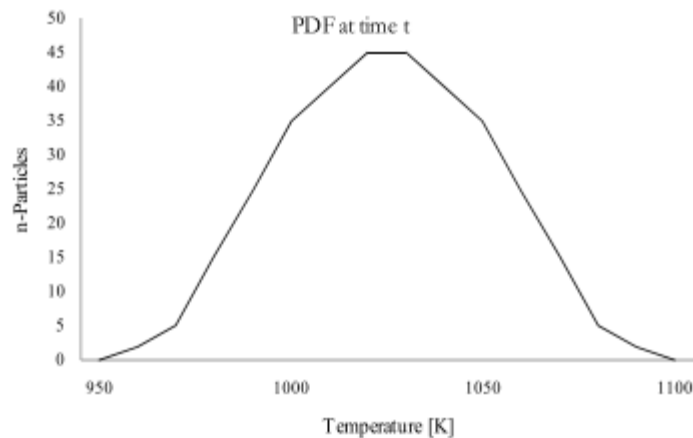


Figure 3.1 Example of PDF shape for Temperature (Tunér 2011).

Figure 3.1 shows a theoretical bell-shaped PDF for temperature, where the largest numbers of particles have temperatures of 1010-1040 K, and no particles have temperatures below 950 K or above 1100 K. During calculations with the SRM, the shape of the PDFs and their range of the variables change with each time step.

This approach consists of a cylinder gas mixture which is separated into visionary particles. According to this approach, particles which represent the mass density from the PDF are defined by the user.

When the model is described, between global and local quantities are defined. The global quantities are total mass, m , volume, $V(t)$, mean density, $\rho(t)$, and pressure, $p(t)$. It is assumed that global quantities do not vary spatially in the combustion chamber.

Local quantities are chemical species mass fractions, $Y_i(t)$, $i=1, \dots, S$, and the temperature $T(t)$. They can vary within combustion chamber and are assumed to be random variables. In PDF method, initially random variable has to be defined from particles in the fuel mixture. After defining the random variable (Φ_1, \dots, Φ_N) , realizations of this variable are stated as $(\psi_1, \dots, \psi_{S+1}, t)$ which represents the sample space variables of corresponding random variables. After finding the sample space variables (realisations), their corresponding joint scalar mass density function (MDF) can be calculated as ' $F_\Phi(\psi_1, \dots, \psi_{S+1}, t)$ '.

The time evolution of the MDF has been assumed statistically homogeneity as well as the partially stirred plug flow reactor model, and it is given by the following MDF transport equation. The governing Equation is 3.1.

$$\frac{\partial}{\partial t} F_\Phi(\psi, t) + \frac{\partial}{\partial \psi_i} ((Q_i(\psi) F_\Phi(\psi, t))) = \text{mixing term} \quad (3.1)$$

The right hand side of the Equation 3.1 describes the mixing of the scalars due to turbulent diffusion. In the left hand side of the Equation 3.1 describes conservation equations for energy and mass as stated by the Navier-Stokes equations for reactive flow. (Barkhudarov et al. 2011).

The initial conditions are given as $F_\Phi(\psi, 0) = F_\Phi^0(\psi)$.

The ψ gives the changes of the MDFs due to chemical reactions, heat transfer and volume work. Q_i denotes the source term for variable ψ .

$$Q_i(\psi) = \frac{M_i}{\rho} \omega_i(\psi), \quad i = 1, \dots, S \quad (3.2)$$

M_i denotes to molar mass, ρ is the density, and ω_i is molar production in Equation 3.2. The ideal gas law can always be considered.

$$Q_{S+1}(\psi) = \frac{1}{c_p} \sum_{i=1}^S h_i \frac{M_i}{\rho} (\psi) - V \frac{1}{c_p} \frac{dP}{dt} - \frac{h_g A}{c_p} (T - T_\omega) \quad (3.3)$$

The convective heat transfer coefficient, h_g is obtained from Woschni equation. V and T_ω represent the instantaneous cylinder volume, and the cylinder wall temperature respectively. The pressure is given by the ideal gas law. The mean temperature and the expected molecular mean weight according to the MDF is used. These equations as well as the transport equation of the MDF have to be solved simultaneously.

In order to apply a stochastic heat transfer step, the original Equation 3.1 has been modified to Equation 3.4. According to this modification, Q_i is distinguished as U (heat transfer step), and G_i (chemical kinetic step) in Equation 3.4. U and G_i is described in Equations 3.5 and 3.6 (Bhave et al. 2006).

$$\begin{aligned} \frac{\partial}{\partial t} F_\phi(\psi, t) + \frac{\partial}{\partial \psi_i} \left((G_i(\psi) F_\phi(\psi, t)) + \frac{\partial}{\partial \psi_{S+1}} (U(\psi_{S+1}) F_\phi(\psi, t)) \right) \\ = \text{mixingterm} \end{aligned} \quad (3.4)$$

$$U = - \frac{h_g A}{m c_p} (T - T_\omega) \quad (3.5)$$

$$G_i = \frac{M_i}{\rho} \omega_{i,j}, \quad i = 1, \dots, S \quad j = 1, \dots, r \quad (3.6)$$

$$G_{S+1} = \frac{1}{c_p} \sum_{i=1}^S h_i \frac{M_i}{\rho} \omega_{i,j} - V \frac{1}{c_p} \frac{dP}{dt} \quad (3.7)$$

To introduce a fluctuation, the third term of Equation 3.4, which is heat transfer part, is replaced by a finite difference scheme:

$$\frac{1}{h} (U(\psi_{S+1}) F(\psi, t) - U(\psi_{S+1} - h) F(\psi_1, \dots, \psi_S, \psi_{S+1} - h, t)), \text{ if } U(\psi_{S+1}) < 0$$

$$\frac{1}{h} (U(\psi_{S+1})F(\psi, t) - U(\psi_{S+1} - h)F(\psi_1, \dots, \psi_S, \psi_{S+1} + h, t)), \text{ if } U(\psi_{S+1}) > 0$$

The fluctuation in temperature is denoted as h which is modeling parameter in temperature and the mixing term of scalars as a result of turbulent diffusion (Barkhudarov et al. 2011)

3.2.1. Operator Splitting and Numerical Solution

To simplify the solving of Equation 3.4, an operator splitting approach is employed at each time step.

The differential operator is decomposed and the parts of the differential operator describing the different physical processes are solved sequentially.

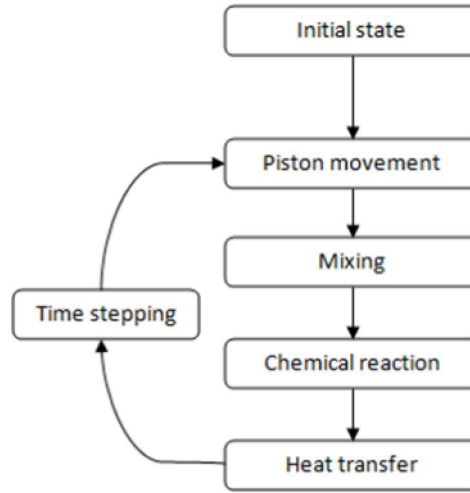


Figure 3.2. The steps in the operator splitting algorithm.(Barkhudarov et al. 2011)

The resulting partial differential equation (PDE), is presented by Equation 3.8.

$$\begin{aligned} \frac{\partial}{\partial t} F_{\phi}(\psi, t) = & \frac{\partial}{\partial \psi_{S+1}} \left(V \frac{1}{c_p} \frac{dp}{dt_{\Delta v}} F_{\phi}(\psi, t) \right. \\ & + \\ & \frac{C_{\phi} \beta}{\tau} \left(\int_{\Delta \phi} F_{\phi}(\psi - \Delta \phi, i) F_{\phi}(\psi + \Delta \psi) d(\Delta \psi) - F_{\phi}(\psi, t) \right) \\ & \left. + \frac{\partial}{\partial \psi_{S+1}} \left(V \frac{1}{c_p} \frac{dp}{dt_{mix}} F_{\phi}(\psi, t) \right) \right) \end{aligned} \quad (3.8)$$

$$\begin{aligned}
& \frac{\partial}{\partial \psi_{S+1}} \left(\frac{1}{c_p} \sum_{i=1}^s h_i \frac{M_i}{\rho} \omega(\Phi) F_\phi(\psi, t) \right) - \sum_{i=1}^s \frac{\partial}{\partial \psi_t} \left(\frac{M_i}{\rho} \omega(\Phi) F_\phi(\psi, t) \right) \\
& \quad + \left(V \frac{1}{c_p} \frac{dp}{dt_{chem}} F_\phi(\psi, t) \right) \\
& \quad - \\
& \frac{\partial}{\partial \psi_{S+1}} \left(\frac{h_g A}{c_p} \psi_{S+1} - T_\omega \right) F_\phi(\psi, t) - \frac{\partial}{\partial \psi_{S+1}} \left(V \frac{1}{c_p} \frac{dp}{dt_{heattr}} F_\phi(\psi, t) \right)
\end{aligned}$$

The pressure assumed constant and the MDFs are updated at each step. In order to ensure the thermodynamic conditions, which are valid for the next operator, pressure correction is performed at the end of each step.

In operator splitting approach, initial conditions are applied at the closing of intake valve. These conditions include global temperature, pressure, cylinder wall temperature, air/fuel ratio etc. At the initialization, the mass within the cylinder is divided into an arbitrary predefined number of particles.

The mixing of particles, heat transfer, chemical reactions and piston movement are solved sequentially at each time step, and the cylinder pressure is recalculated after each time step so that all particles can have the exactly same pressure, since a small error can be occurred when solving different steps in loop at constant pressure (Yang 1998).

According to Equation 3.4. It means that the term concerning the pressure change has to be divided into subterms with respect to each split event, according to Equation 3.9.

$$-V \frac{1}{c_p} \left(\frac{dp}{dt} \right) \quad (3.9)$$

Subterms, which are stated in Equation 3.9, are considered as mixing, heat, piston movement, and these terms are solved with pressure correction.

$$-V \frac{1}{c_p} \left(\frac{dp}{dt} \right) = -V \frac{1}{c_p} \left(\frac{dp}{dt} \right)_{piston} - V \frac{1}{c_p} \left(\frac{dp}{dt} \right)_{mix} - V \frac{1}{c_p} \left(\frac{dp}{dt} \right)_{chem} - V \frac{1}{c_p} \left(\frac{dp}{dt} \right)_{heat}$$

Particles in a system such as i , ($i = 1, \dots, n$), have its own species composition and temperature, giving individual specific heat ratios γ_i and pressures p_i .

In the pressure correction model, pressure equalises for all particles in the system through adiabatic compression.

$$P_i V_i^{\gamma_i} = \bar{P} (V_i + \Delta V_i)^{\gamma_i} \quad (3.10)$$

The adiabatic exponents of the particles are assumed to be constant. In order to solve \bar{P} , the sum of the volume of all particles are considered equal to the total cylinder volume, and adiabatic exponents of particles are also assumed as constant.

After pressure correction is applied in the loop, temperature and density of all particles are updated with respect to the new pressure.

$$\sum_{i=1}^n V_i \left(\frac{P_i^{\gamma_i}}{\bar{P}} \right)^{\frac{1}{\gamma_i}} = V_{total} = V_{cylinder} \quad (3.11)$$

3.2.2. Piston Movement

The piston movement should be considered as well in the SRM. Air and fuel are compressed and combusted as a mixture in a piston cylinder engine. After air/fuel combusts with piston movement, expansion occurs. This leads the heat to convert into work and the exhaust gases pump out.

Closed engine cycles can be modelled in SRM with LOGEsoft. In the closed cycle, the piston movement works against the closed cylinder, which causes to decrease the volume while pressure is increasing. The piston movement is the main step in order to predict compression, combustion and expansion parts.

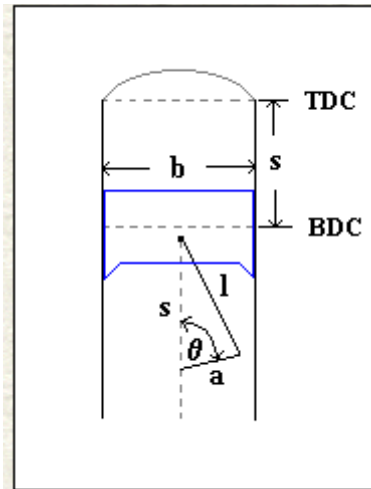


Figure 3.3 Piston Cylinder.

The volume of the piston cylinder can be determined as a function of crank angle from the compression ratio, the stroke, bore and connecting rod length. The geometric parameters of the piston cylinder are represented in Figure 3.3 where b is the bore, s is the stroke, l is the connecting rod length, a is the crank radius ($\frac{1}{2} s$), θ is the crank angle, TDC is the top dead center, and BDC is the bottom dead center.

At a given crank angle the volume is given in Equation 3.12.

$$V = V_c + \frac{\pi}{4} b^2 x \quad (3.12)$$

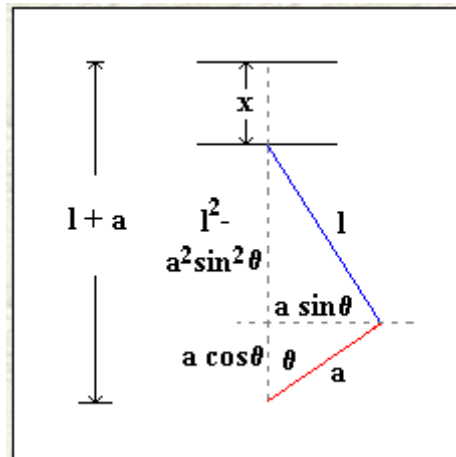


Figure 3.4 Geometric solution for x .

$$x = a + l - [(l^2 - a^2 \sin^2 \theta)^{1/2} + a \cos \theta] \quad (3.13)$$

The compression ratio is defined as the ratio between the maximum and minimum volume, $r = V_1/V_0$. For Otto ignition $r = 10$ and for a diesel engine the

compression ration varies from 12 to 24. Substituting the maximum volume with the displacement volume yields:

$$\begin{aligned} r &= 1 + V_d / V_c \\ V_c &= V_d / r - 1 \end{aligned} \quad (3.14)$$

Substituting Equations 3.13 and 3.14 into Equation 3.12, results in the following relationship for the cylinder volume is given in Equation 3.15 where $R=1/a$

$$V = \frac{V_d}{r-1} + \frac{V_d}{2} (1 + R - \cos\theta - (\sqrt{R^2 - \sin^2\theta})) \quad (3.15)$$

3.2.3. Chemical Reactions

The equation 3.16 should be solved during the chemistry step. The backward differentiating function (BDF) method is combined with a newton algorithm to solve the governing equations since they are highly non-linear.

$$\frac{\partial}{\partial t} F \Phi = \frac{\partial}{\partial \psi_{s+1}} \left(\frac{1}{C_p} \sum_{i=1}^s h_i \frac{M_i}{\rho} \omega(\Phi) F \Phi(\psi, t) \right) - \sum_{i=1}^s \frac{\partial}{\partial \psi_i} \left(\frac{M_i}{\rho} \omega(\Phi) F \Phi(\psi, t) \right) \quad (3.16)$$

The result is the new chemical composition for the particles on the new step.

3.2.4. Heat Transfer

The gas in-homogeneties can be modelled realistically with SRM. The in-homogeneties occur from fuel injection for DI engines. The in-homogeneties occur from in coming gas for all engines due to the heat exchange with cylinder walls. Therefore heat transfer model should be applied.

The Woschni heat transfer model is applied in SRM in order to determine the amount of heat to transfer. Heat transfer through the cylinder side walls is an important process in determining overall performance, size and cooling capacity of an internal combustion engine (ICE). It affects the indicated efficiency, because it reduces the cylinder temperature and pressure, and decrease the work transferred on the piston per

cycle. The heat loss through the walls is in the range of 10–15% of the total fuel energy supplied to the engine during one working cycle. In particular, the Woschni correlation has frequently been used in the heat transfer studies with proper constants in today's SI and diesel engines, and also it has been correlated for HCCI engines recently. Instantaneous heat transfer coefficient that is adopted from Woschni is calculated in Equation 3.17

$$h(\theta) = 3.26P(\theta)^b T_g(\theta)^{0.75-16.2b} D^{b-1} w(\theta)^b \quad (3.17)$$

He assumed the “*b* exponent” as 0.8, and he emphasized that effective gas velocity, *w*, consists of two contributions in Equation 3.17. The first contribution is scaled with mean piston motion and swirl, and the second contribution is related to turbulence effects and ΔP pressure rise which is resulted from combustion. The second contribution also includes the influence of radiation.

In this model, the average cylinder gas velocity, *w*, determined for a four-stroke, water cooled, valve direct injection CI engine without swirl is defined as equation. (3.18).

$$w = \left[C_1 \bar{S}_p + C_2 \frac{V_d T_r}{p_r V_r} (p - p_m) \right] \quad (3.18)$$

V_d is the displaced volume, *p*, is the instantaneous cylinder pressure p_r , V_r , T_r are the working fluid pressure, volume, and temperature at some reference state such as start of combustion or inlet valve closing. P_m is the motored cylinder pressure at the same crank angle as *p*. Accordingly, $C_1 = 2,28$ and $C_2 = 3.24 \times 10^{-3}$ for the combustion, and expansion period.

In the implementation of the heat transfer model in LOGEsoft, the area of the each surface (A^i) is calculated as assigned temperature (T_w^i) according to the current piston position. Then, the total heat transfer (Q^i) for surface (*i*) and time step are calculated according to the woschni correlation. *Ch* is a stochastic, heat transfer constant which is described from the user and *N* refers to the total number of particles. For a random particle, *n*, heat transfer through the fluctuation in heat between the particle and the wall are calculated.

$$h_n = \frac{T_n - T_w^i}{C_h}$$

$$T_n = T_w^i - h_n \quad (3.19)$$

A low stochastic constant, (C_h) causes more amount of heat transfer for distribution rather than a high C_h . The homogeneous engine model can be produced by higher C_h which goes to infinity (Przyby and Postrzednik 2013).

3.2.5. Heat Release Calculation

The heat release rate refers to “the sum of chemical heat release from each particle over one CAD step”, as stated by Equation 3.20. which is an important result parameter.

$$HRR = \sum_{n=1}^N m_n \frac{(H_n^f - H_n^i)}{\Delta CAD} \quad (3.20)$$

where n refers to the particle index, m is the particle mass, H^f defines the enthalpy of the particle after the chemistry step, and H^i refers to the particle enthalpy before the chemistry step.

3.3. Direct Injection Models

In this study, DI model is applied with SRM. The LOGEsoft DI-SRM contains two different fuel injection models. The first one employs a separate vaporization ratesto depending on engine conditions which is called as spray vaporization model. The second one assumes all injected fuel vapourised instantly. This is called as the instantaneous vaporization model which is used in this study.

3.3.1. Instantaneous Vaporisation Model

The injected fuel is assumed to be vapourised instantaneously at the moment of injection in this model. The only difference is that expanding operator splitting loop to include fuel injection part (Figure 3.5).

The energy needed for vaporization of injected fuel should be considered. In the simulations, the vaporised amount to be injected is determined by a linear interpolation.

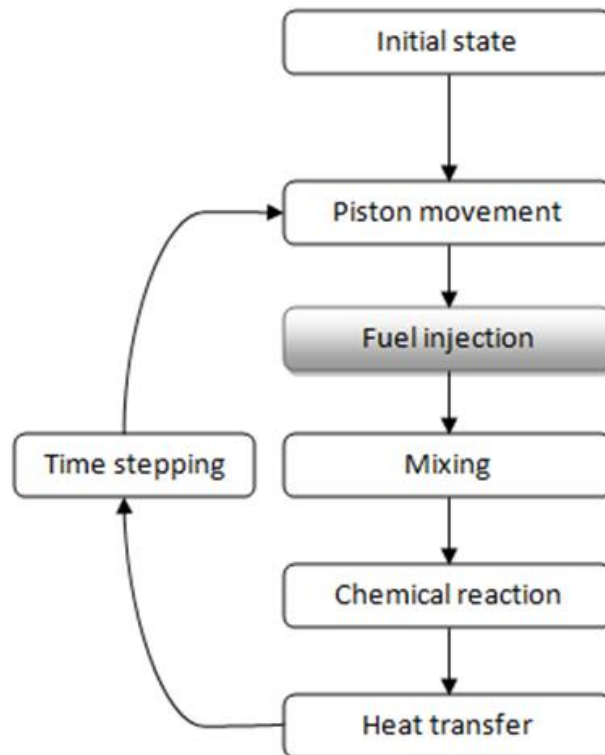


Figure 3.5. Operator split loop for the DI SRM including the fuel injection step (Barkhudarov et al. 2011).

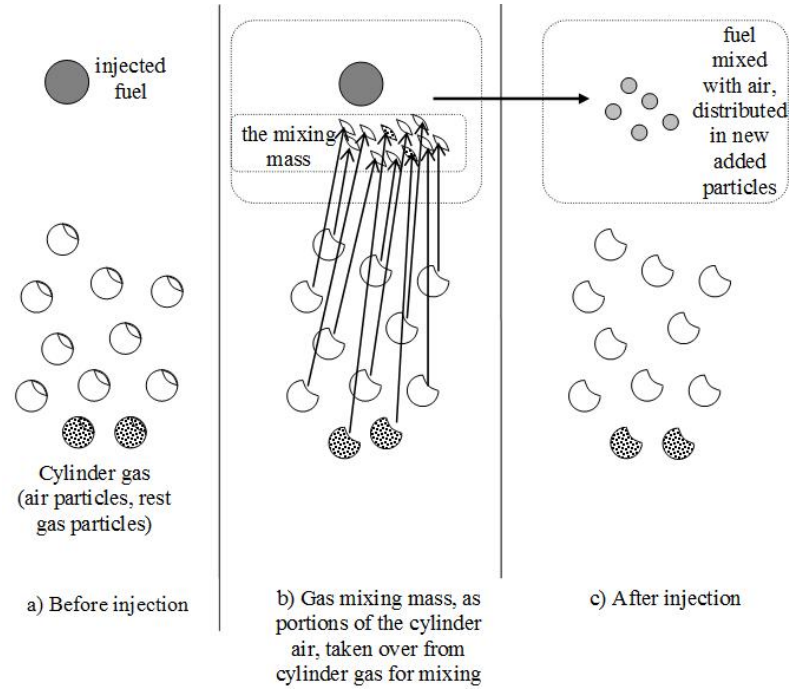


Figure 3.6 When fuel m_f is added to the cylinder, the mass fractions and temperatures (Curl, 1963).

The mixing mass is taken from the already existing particles and it is combined with the mass of injected fuel, then to form new particles. When fuel is added into the cylinder, m_f , current particles' temperature and mass fractions are changed due to the composition of fuel and its liquid injection temperature. Therefore, the source term of the global differential equation needs to be extended (Barkhudarov et al. 2011).

$$\begin{aligned}
 G_i^{inj} &= \frac{m_f}{m} (Y_{i,f} - Y_i), \quad i=1, \dots, S \\
 G_i^{inj} &= \frac{m_f}{m} (M_{i,f} - M_i), \quad i=S+1, \dots, S+n_m-1 \\
 G_{S+n_m}^{inj} &= \frac{1}{\rho C_p} \frac{m_f}{V} \sum_{i=1}^S Y_{i,f} (h_{i,f} - h_i)
 \end{aligned} \tag{3.21}$$

G_i^{inj} , chemical kinetic for injection particles, $S + n_m$ is the index of the temperature. m is the total mass of the cylinder gas, and changes in accordance with the added fuel. The mixing mass is taken from the existing cylinder gas particles. Figure 3.7 presents a schematic for the redistribution of mass and species in a particle after a certain portion of it, represented by a dashed line, has been removed and used for fuel mixing. A given species (i), represented by the gray field.

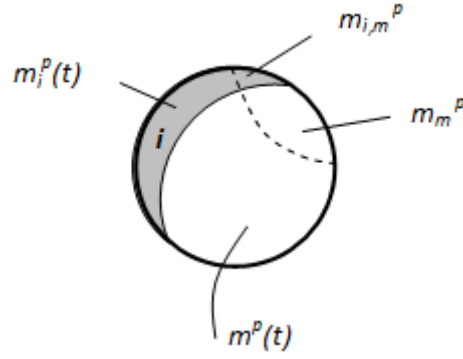


Figure 3.7 Schematic of an existing particle and of the ratios of masses transferred from it during fuel injection (Curl. 1963)

In Figure 3.7 is proportionally distributed between the remaining particles and the mass collected for mixing with the fuel. If $(m_{i,m}^p)$ denotes the mass of species, (i) taken from particle, (p) as contribution to the mixing mass, the updated mass fraction ' $Y_i^p(t + \Delta t)$ ' of i in particle p is

$$Y_i^p(t + \Delta t) = \frac{m_i^p(t) - m_{i,m}^p}{m_p(t) - m_m^p}, \quad p = 1, \dots, N \quad (3.22)$$

The new and added particles all have identical species mass fractions

$$Y_i^p(t + \Delta t) = \frac{m_{i,f} - m_{i,m}}{m_f - m_m}, \quad p = N + 1, \dots, N' \quad (3.23)$$

where $(m_{i,m})$ is the mean mass of species i for the present particles. The updated temperatures ' $T_i^p(t + \Delta t)$ ' of the old and new particles, respectively, are:

$$\begin{aligned} T_i^p(t + \Delta t) &= T^p(t), & p &= 1, \dots, N \\ T_i^p(t + \Delta t) &= T_v, & p &= N + 1, \dots, N' \end{aligned} \quad (3.24)$$

Pressure is assumed constant during vapourisation and the injected fuel is assumed to have the same pressure as the cylinder gas. As constant pressure implies constant enthalpy and since the resulting temperature of the gas mixture is known, the gas mass needed to vapourise the fuel, (m_{mv}) can be calculated through Equation 3.25.

$$m_{mv} = \frac{h_{f,liq}(T_f) - h_{f,gas}(T_v)}{h_m(T_v) - h_m(T_m)} m_f \quad (3.25)$$

The subscript, (*f*) denotes the injected fuel and (*v*) vaporisation. If the fuel is a mixture of several different species, Equation 3.25 is applied to each species in turn as each species has its own vaporisation temperature (Barkhudarov et al. 2011).

3.4. Surrogate Fuels

Although a surrogate fuel does not necessarily need to contain all components that are representative of the molecules contained in diesel fuel, it is reasonable to expect that a compositional match may permit.

It must be noted however that the most of the presented work on surrogate fuels is heavily biased in order to cover chemical kinetics first. The physical properties of surrogates are important as much as chemical mechanisms for larger molecules. The choice of fuel as a single component or blended mixture, is based on the targets that one is interested in.

Table 3.1. Typical Diesel fuel composition

Group	EU Diesel
Alkanes/Alkenenes	25-50
Cyclo-Alkanes	20-40
Aromatics	15-40

Property targets refer to fundamental physical and chemical fuel properties. The physical and chemical complexity of a surrogate fuel are reduced compared to that of a commercial diesel fuel. In general, it is possible to match a wide range of properties such as viscosity, chemical composition and surface tension with a single surrogate formulation. In the studies with blended surrogate fuels, several group contribution methods are available and can be applied to desired property targets. Table 3.2 shows a comparison of relevant different fuel properties. Most of the surrogate fuel properties that are based on the chemical compositions are simply calculated. According to these properties and earlier presented measurement results, expectations of the behavior of n-heptane as a surrogate fuel for diesel are formulated.

Table 3.2 Properties of diesel, n-heptane & IDEA fuel.

Variable	diesel	n-heptane	IDEA	Unit
Cetane number	56	56	56	-
Boiling point / range	483-634	372	447-518	K
Lower Heating Value	41.54	44.6	42.3	MJ/kg
AF stoichiometric	14.7	15.4	14.45	-
C ratio	86.2	30.4	37.1	Molar%
H ratio	13.3	69.6	62.9	Molar%
O ratio	0.5	0	0	Molar%
C/H ratio	1.85	2.286	1.70	-
Molar mass	170	100	142	kg/kmol

3.4.1. N-Heptane

Depending on the application target, a single component surrogate may suffice. N-heptane (N-C₇H₁₆) is a gasoline-range single component surrogate diesel fuel. Since the n-heptane cetane number is quite similar with current European and Japanese diesel fuel, it is usually preferred for computational studies. Additionally, detailed chemical-kinetic mechanisms for low, intermediate, and high temperature n-heptane oxidation are easily available. Several models exist to have sufficiently reduced number of species and reactions for n-heptane, and it can be used in CFD simulations or any other computational tool.

Table 3.3 Properties of diesel, n-heptane, toluene fuel.

Property	Diesel	Heptane	Toluene
Chemical formula	C _n H _{1.8n}	C ₇ H ₁₆	C ₇ H ₈
Density (kg/m ³)	827-840	680	867
Cetane number	52	55	0

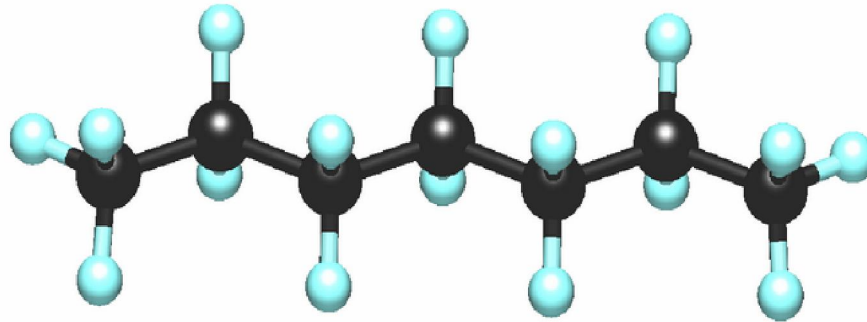


Figure 3.8 Molecule structure of n-heptane (C_7H_{16}).

According to n-heptane characteristic and easy implementation by numerical tools, it has been chosen as the first surrogate fuel in order to compare results with experimental diesel data.

3.4.2. Finding proper heat transfer coefficient

The purpose of the present research is to test different surrogate fuels with different injection timings (SOI). In order to achieve the numerical model, experimental conditions were taken as reference. The experimental studies were tested with an optical engine. To minimize the errors due to false phasing of the pressure trace, the top dead center (TDC) position is important, because the heat release calculations were based on individual cycles of the pressure trace. In order to achieve the same TDC pressure, the Woschni heat transfer model was normally tuned with respect to the shape of the heat release curves. However, for this case, the heat release curves motored cylinder pressures were used as HRR were not available. Thus higher heat losses and blow by effects and engine position were accounted for. Since the engine was outside, heat transfer is higher than classical engine operation conditions. When all these conditions are considered, Figure 3.9 is created. Finding proper heat transfer coefficients and matching pressure traces is important, because increasing injection pressure causes to

mixing air and fuel quickly, and limiting the initial rate of HRR keeps NO_x production at the minimum amount.

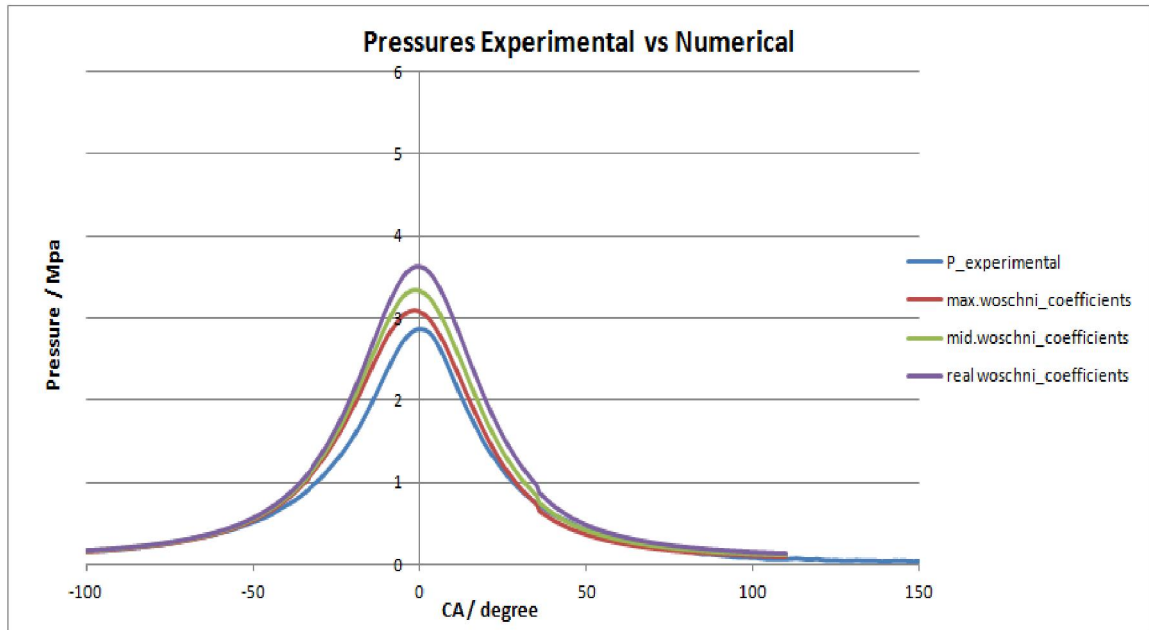


Figure 3.9 Pressure graphs for different woschni heat transfer coefficients.

Three cases were tuned to use proper woschni coefficients due to the blow by effect, higher heat transfer. According to this transfer, $C_1 = 2.28$ and $C_2 = 3.24 \times 10^{-3}$ were taken from real woschni coefficient. In second trial, $C_1 = 8.28$ and $C_2 = 12.24 \times 10^{-3}$ (which is described as mid.woschni_coefficients in (Fig.3.9) and finally $C_1 = 16.28$ and $C_2 = 20.24 \times 10^{-3}$ were found proper for the model in the HRR calculations. After finding the best matching for engine conditions, all simulations were tested with same model.

CHAPTER 4

RESULT AND DISCUSSION

In this study, surrogate fuel blends were tested by using a computational tool which named LOGEsoft. The tool was based on the SRM in DI engines. Event though SRM can be used for 1-D, 2-D or 3-D calculations, the spatial zero dimensional model was chosen in this study, which was proper for the reaction engineering. The species were presented in spatially in chemical reactions. The mathematical modelling was based on the probability density function (PDF) approach. Chemical kinetics and heat transfer for species in the cylinder were considered in this approach. Since the governing equations are highly non-linear, sub cycles had to be implemented into the governing equations. A standard backward differential function method combined with a Newton algorithm was used to solve this system of equations.

At the end of the simulations, before presenting the results, the model was compared with the existent experimental results. For validation purposes, however, there were not so many references related with the LOGEsoft and the same working conditions utilized in this study. It was observed that the trends of the distributions of ignition delays and temperature are mostly consistent with the results of this study. Nevertheless, it is still necessary to perform quantitative comparison and more test with different surrogate fuels.

4.1. Experimental Study

Experimental investigations were performed by Diez, Løvås, and Crookes (2012). The experiments were performed in an optical combustion chamber. The engine is run on standard diesel fuel. The same engine specifications were utilized for inputs in the LOGEsoft. Figure 4.1 shows the schematic diagram of the optical engine and in Table 4.1 engine specifications are listed.

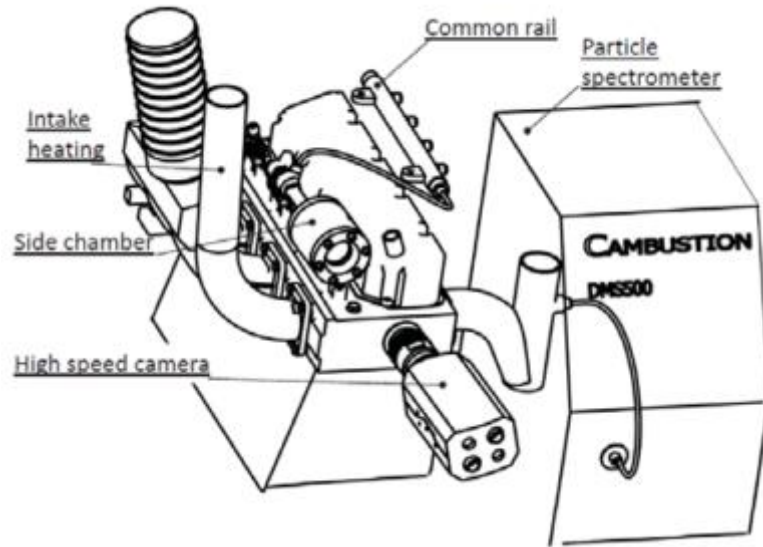


Figure 4.1 The Optical chamber in experiments (Diez, Alvaro and Terese Løvås 2012).

Table 4.1 The Engine specifications.

Engine / Model	Ford / In-line O.H.V
Number of cylinders	4
Bore diameter /m	0.09367
Stroke /m	0.09054
Connecting rod length /m	0.1539
Crank length (m)	0.04527
Clearance volume / 10^{-6} m^3	34.66
Engine capacity / 10^{-3} m^3	2.496
Compression ratio	16.9
Swirl ratio	2.1
Injection timing	15, 20, 25, 30, 35
Engine Speed for Experiments r/min	1020
Equivalence ratio for all experiments	0.4
Injection duration for all experiments / ms	0.66
Initial Crank Angle / degree	-113
Final Crank Angle / degree	110

The model is developed following the engine specifications. In addition to this, for the simulation, some parameters such as cylinder wall temperature and heat transfer coefficients have to be defined as inputs. The determination of the Woschni heat

transfer coefficients were explained in the last part of methodology. It is important to remember that, since the optical combustion chamber is outside, heat loss must be considered higher.

The experimental results for diesel were obtained according to cylinder pressure data and luminosity.

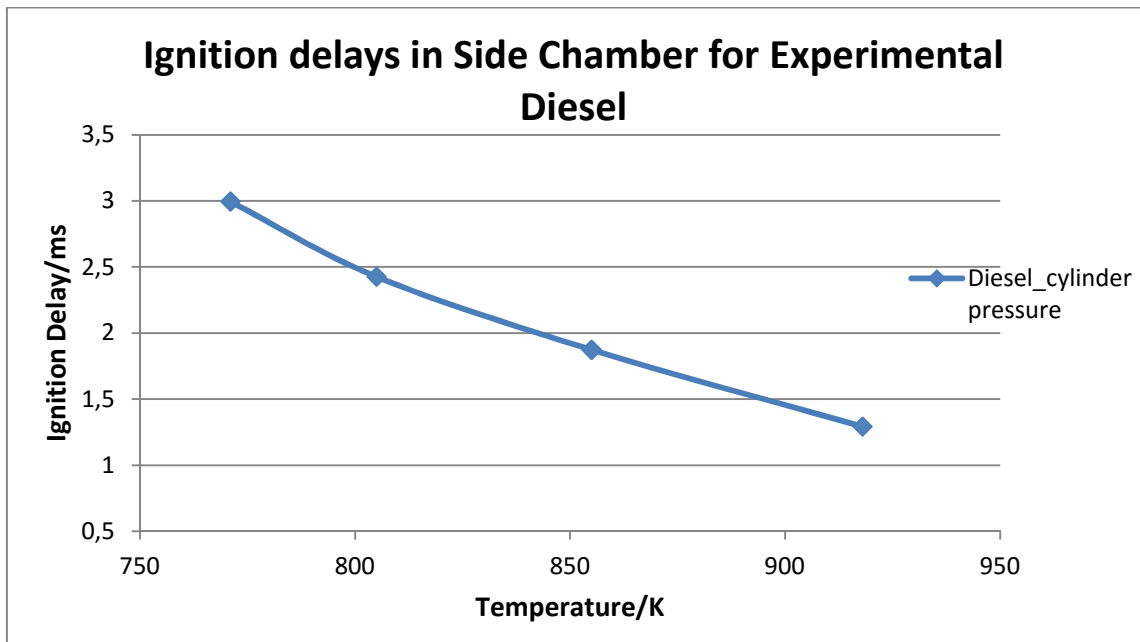


Figure 4.2 Ignition delays for experimental diesel results related to cylinder pressure.

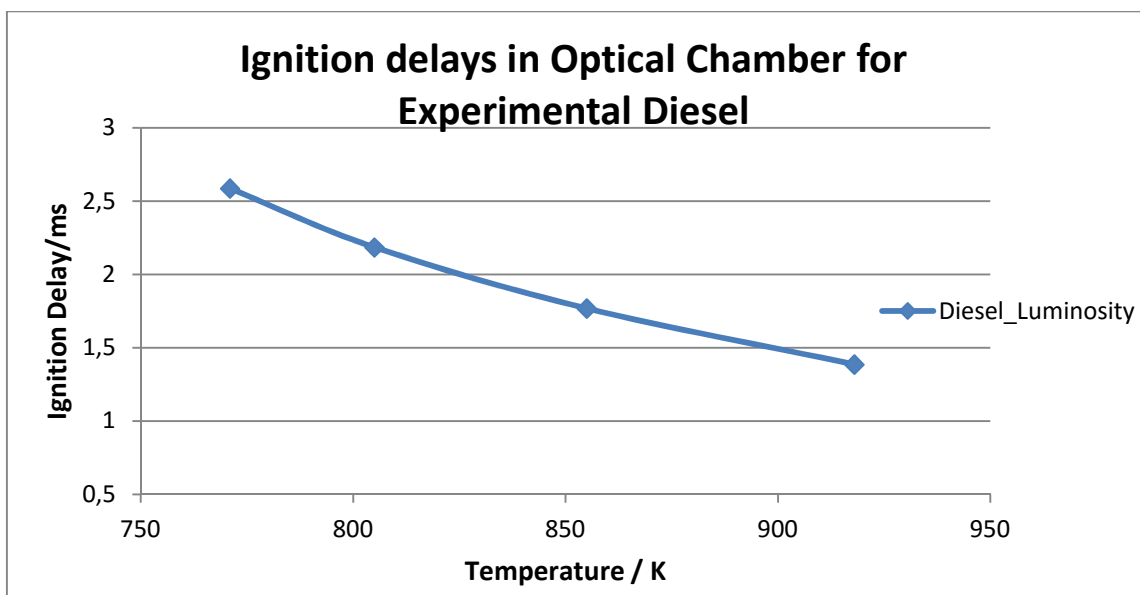


Figure 4.3 Ignition delays for experimental diesel results related to luminosity.

4.2. Ignition Delay Definition

The ignition delay time of diesel cycle engines is a fundamental parameter to effectively control the combustion process. The ignition delay time is influenced by several physicochemical phenomena associated with the nature of the fuel, such as molecular structure, volatility, viscosity, surface tension, and mechanical characteristics of the engines, such as compression ratio, pressure of the injection system, and injection angle. Ignition delay is the time interval between the start of fuel injection (SOI) and the start of combustion (SOC). Ignition delay results are often presented in Arrhenius expression. The Arrhenius expression for the ignition delay is given in equation (3.26).

$$\tau = A \exp\left(\frac{E}{RT_a}\right) \quad (3.26)$$

Where τ is the ignition delay in (ms) and T_a is the ambient temperature at the moment of the fuel injection. A is the exponential constant, E the global activation energy and R the universal gas constant.

In order to calculate ignition delay and convert the results to millisecond (ms) the method is given in equation (3.27)

$$t = \frac{\text{angle the crank travels through}}{6 \times RPM} \quad (3.27)$$

Where RPM is revolutions of crank per minute and t is the time in seconds (s) that the crank takes to travel the angle. It has to be converted to ms. Angle that the crank travels through is calculated from difference between SOI and SOC.

4.3. Examined Fuels

A single molecule long chain hydrocarbon which is n-heptane was chosen as one of the main components of diesel fuel. N-heptane can be sufficient for simple applications like combustion efficiency. However, more complex surrogates will be

required for chemistry dependent applications, such as soot formation or combustion phasing, radiation loading, combustion staging, or lean, premixed, and prevaporized applications. A model of such a complex surrogate blend means that there is one master mechanism that includes combustion models for all the fuel components considered. Components of sub mechanisms must be stable in terms of common reactions and reaction rates, and species thermodynamic properties. Components the fuel blended regarding to match one or more targets, such as combustion, NO_x emissions, sooting behavior, and physical properties. Matching the emissions behavior of a real fuel requires more complex mixtures. Adding components from various fuel classes, such as aromatics, cyclic alkanes, olefins, is necessary to match the emission targets.

In this study, ignition delay and soot formation results were presented for n-heptane and mixtures of n-heptane / toluene and n-heptane / isooctane. N-heptane was chosen as first surrogate fuel, since it is a gasoline range molecule and n-heptane's cetane number (CN) is comparable with diesel fuel. Cetane number denotes the ignition delay time. Ignition delay period starts with the injection of fuel and consists of physical and chemical delay periods until the autoignition occurs. The cetane number ranks the fuels; the higher cetane number is, the faster is the auto-ignition. Fuels with a high CN have a very short ignition delay time; that is, ignition occurs in a very brief interval of time after injection begins. Conversely, the longer the ignition delay time is, the lower is the CN. Accordingly, n-heptane implementation and monitoring is easy to use in computational studies. It is often utilized as a surrogate diesel fuel. More definitions are defined in the methodology part. Toluene was chosen as the second component, since it would act as an aromatic soot promoter. 5 % toluene / 95 % n-heptane, 10 % toluene / 90 % n-heptane, and the last 10 % isooctane / 90 % n-heptane blends were tested as mixtures. In order to find ignition delay and temperature, several runs were made in different injection timings.

For the fuels investigated, different injection timings were analysed and calculated the ignition delays after determining start of injection and start of combustion

In order to predict starting of injection timing N-C₇H₁₆ results were considered.

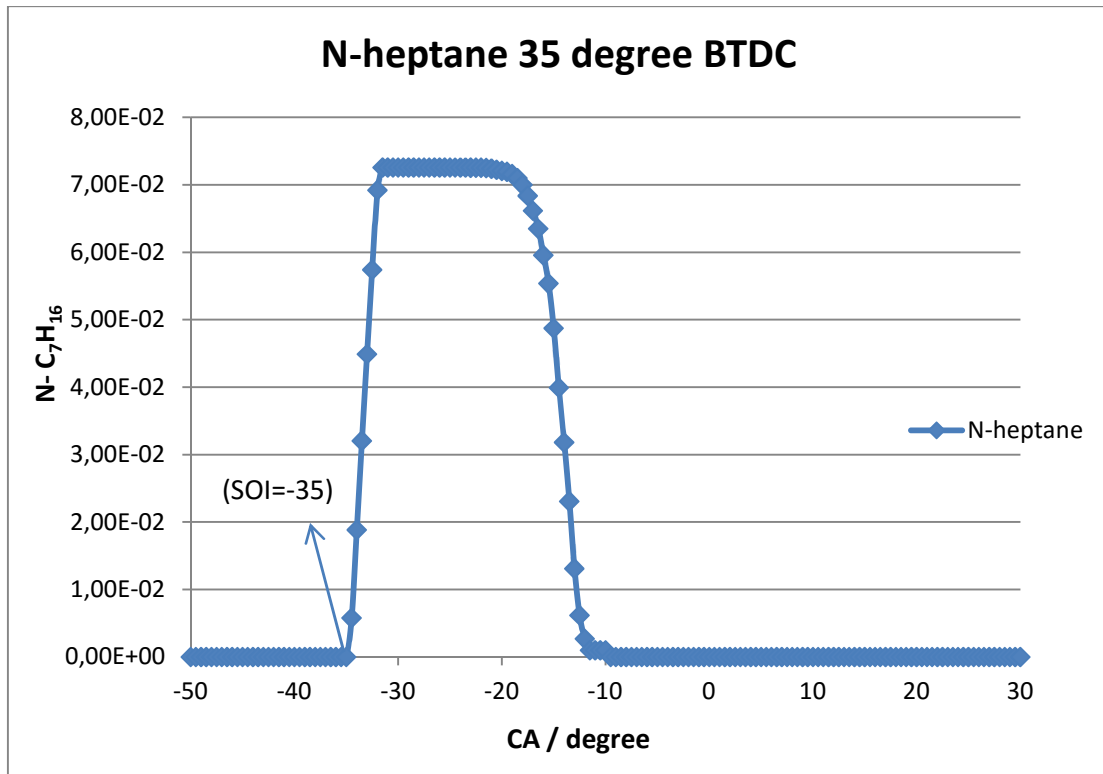


Figure 4.4 Start of Injection N-Heptane value (SOI 35° BTDC).

Figure 4.4 verified that, when the crankshaft made 35 degree before top dead center, the fuel started to be injected. The start of injection timings was identified in the same way for all injection timings and tests.

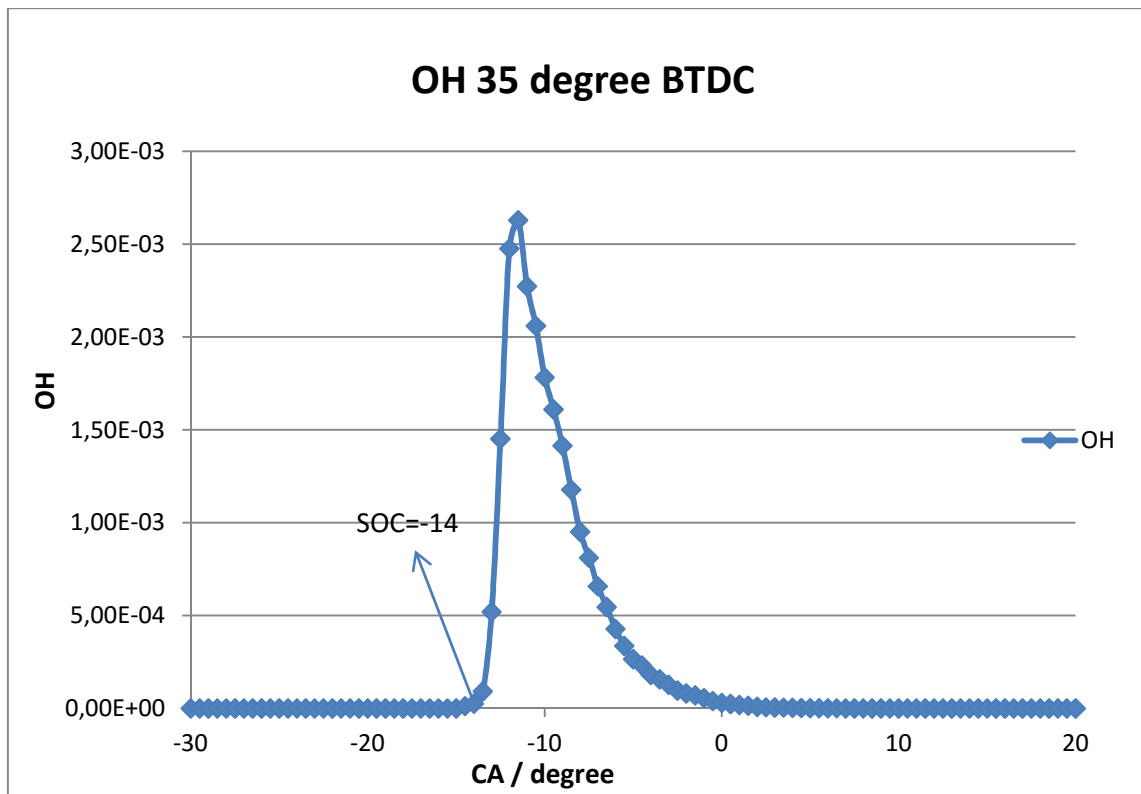


Figure 4.5 Determination of the start of combustion n-heptane (SOC 35° BTDC). .

OH was a marker to understand the start of combustion timings. After fuel injected into the cylinder, combustion initiation take place, so that ignition timings could be detected from OH mass fractions.

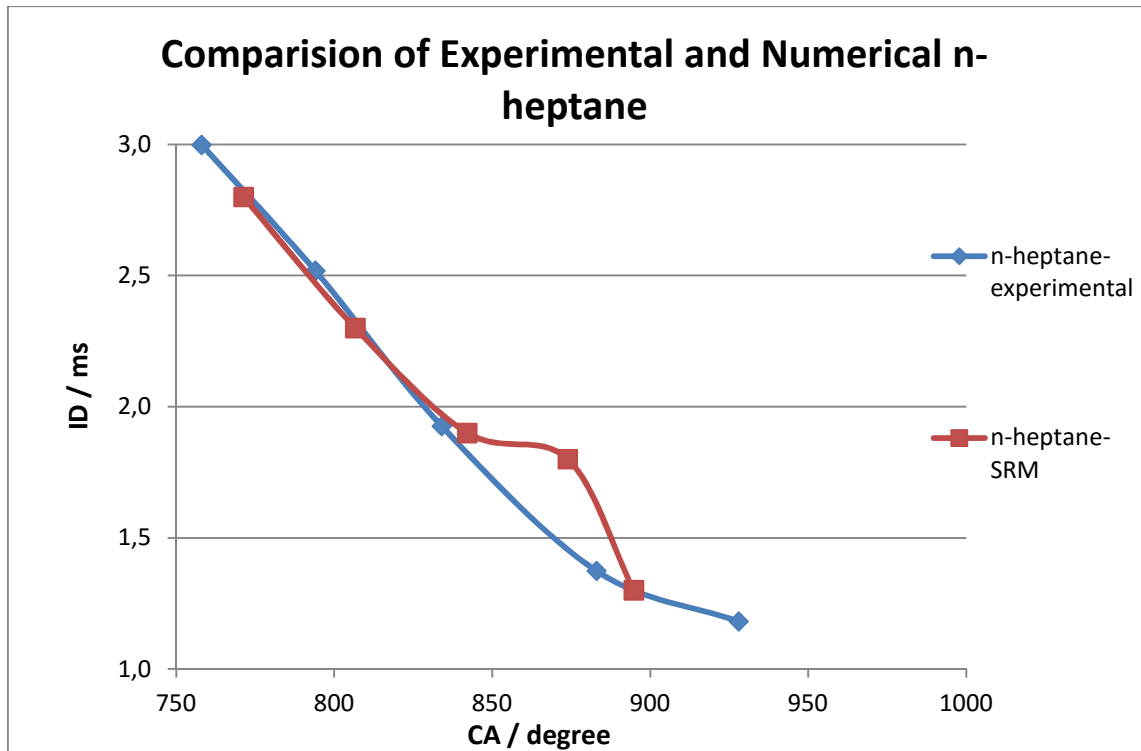


Figure 4.6 Experimental and numerical comparisons of n-heptane.

As a result of the simulation, numerical n-heptane ID was found slightly lower than experimental that was shown in Figure 4.6. One of the reason of this situation could be fuels assumed fully vaporized in cylinder. Evaporating all fuels instantaneously, reduce the time for premixed phase related to lower ignition delay.

In Table 4.2, injection timings were listed for all tested fuels and injection timings. SOI, SOC, temperature and calculated ignition delays have indicated as a result of this study.

Table 4.2 Ignition delays for surrogate fuels.

Fuel blends		N-Heptane	N-Heptane%95 Toluene%5	N-Heptane %90 Toluene%10	N-Heptane %90 Isooctane %10
35 BTDC	SOI	-35	-35	-35	-35
	SOC	-14	-15	-14.5	-15.5
	ID/°CA	21	20	20.5	19.5
	ID/ms	3.5	3.3	3.4	3.3
	Temperature	735.7	735.7	735.7	735.7
30 BTDC	SOI	-30	-30	-30	-30
	SOC	-13.5	-14	-14	-15
	ID/°CA	16.5	16	16	15
	ID/ms	2.8	2.5	2.5	2.5
	Temperature	771.4	771.3	771.3	771.3
25 BTDC	SOI	-25	-25	-25	-25
	SOC	-11.5	-11.5	-11	-12.5
	ID/°CA	13.5	13.5	14	12.5
	ID/ms	2.3	2.3	2.3	2.1
	Temperature	806.8	806.7	806.7	806.7
20 BTDC	SOI	-20	-20	-20	-20
	SOC	-8.5	-8.5	-9	-9
	ID/°CA	11.5	11.5	11	11
	ID/ms	1.9	1.9	1.8	1.8
	Temperature	842.2	842.1	842.1	842.1
15 BTDC	SOI	-15	-15	-15	-15
	SOC	-4.5	-4.5	-4.5	-6
	ID/°CA	10.5	10.5	10.5	9
	ID/ms	1.75	1.8	1.8	1.5
	Temperature	874.1	873.9	873.9	873.9
10 BTDC	SOI	-10	-10	-10	-10
	SOC	-2.5	-2.5	-2.5	-3
	ID/°CA	7.5	7.5	7.5	7
	ID/ms	1.3	1.3	1.3	1.2
	Temperature	894.9	894.8	894.8	894.8

Figure 4.7 and 4.8 represent the comparison graphs for ignition delays of diesel and the surrogate fuels. Surrogate fuels' ignition delays were compared with experimental diesel fuel ignition delays. Since, the experimental studies were performed from both cylinder pressure data and luminosity. The simulation results were plotted separately in order to compare experimental study.

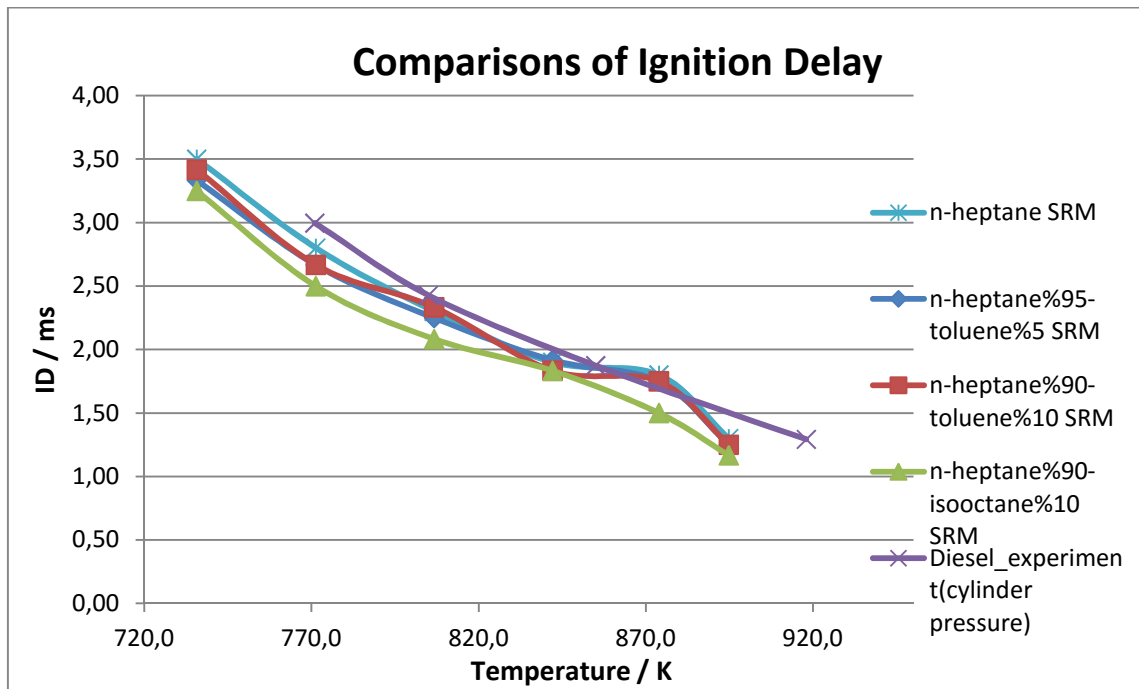


Figure 4.7 Ignition delays comparisons regard to the experimental diesel from pressure.

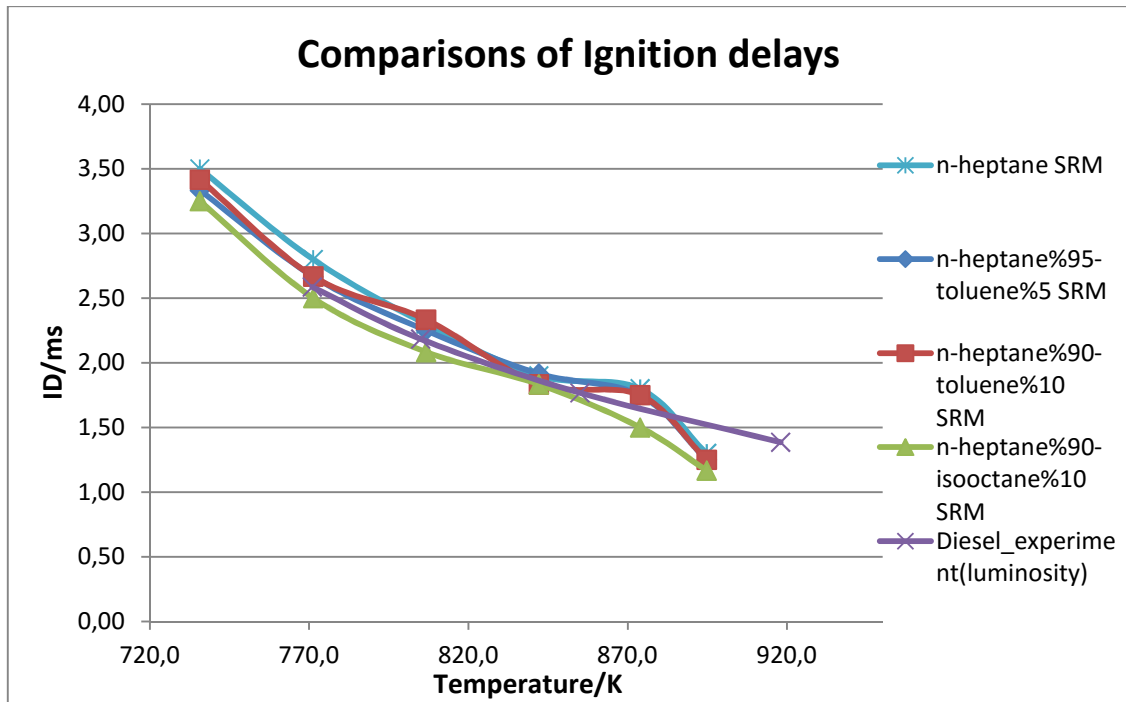


Figure 4.8 Ignition delays comparisons regard to the experimental diesel from luminosity

All tested surrogate fuels showed very similar profiles, even though the ignition delay for the fuels investigated were higher for diesel fuel except n-heptane / isooctane blend. One of the reason for this situation could be isooctane structure. If fuel contain high concentrations of n-paraffins generally, it has low ignition delay times because of the activation energy to form free radicals. Besides, they have stable molecular structures and require high temperatures and pressures to begin combustion. Since the isooctane percentage is not very high, ignition delay fewness is not very significant. Furthermore, the model was developed with regarding to the experimental conditions, a small differences occurred between pressures, which is shown in Figure 4.9. The effects of the high pressure cause to higher temperature in cylinder, and this may be cause to a moderation for ignition delay.

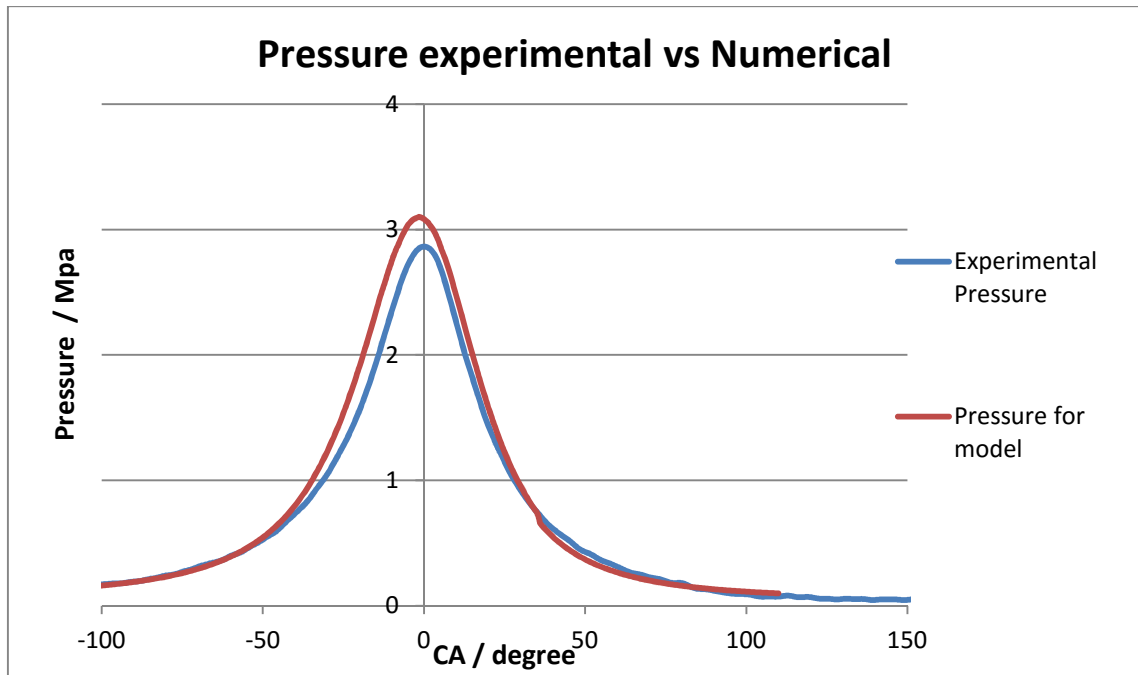


Figure 4.9 Differences between experimental and numerical pressure.

The ignition delay (ID) calculations from cylinder pressure and from luminosity were not exactly the same. The authors explained this as, the SOC is determined from the high temperature reaction in cylinder pressure. Besides, they assumed that the camera could not detect chemiluminescence from the cool flame reaction at specific ignition sites at lower temperatures. For the later injection timings, which is higher temperature, combustion starts at places, and the pressure sensor is recorded easily. Therefore, the differences between the ID from luminosity and the ID from the cylinder pressure detection is higher at early injection timings (at lower temperatures).

Calculated ID were found slightly higher than the experimental diesel results. The reason of this is high heat transfer regarding to the engine conditions. Reducing temperature in cylinder causes to increment in ignition delays. Even though these differences were considered when doing simulations, these small differences can be explained because of the determination of the heat transfer. Adding small amount of toluene does not have a significant effect on ignition delay. Since toluene cetane number is zero and n-heptane cetane number is quite similar with diesel. These results are in agreement with findings in literature (Diez, Løvås, and Crookes 2012). If toluene percentage was kept below 10 vol % in n-heptane and toluene mixtures, they have similar ignition delays (Figure 4.7 and Figure 4.8).

The latest injection timing (SOI 10 °CA BTDC) produces the shortest ignition delay. Late injection timings cause to the shortest combustion in premixed phase when

small particles are formed and more soot producing during the combustion phase. When the injection timing is advanced, longer ID causes to more fuel burning in the premixed phase. Therefore, soot emissions decrease.

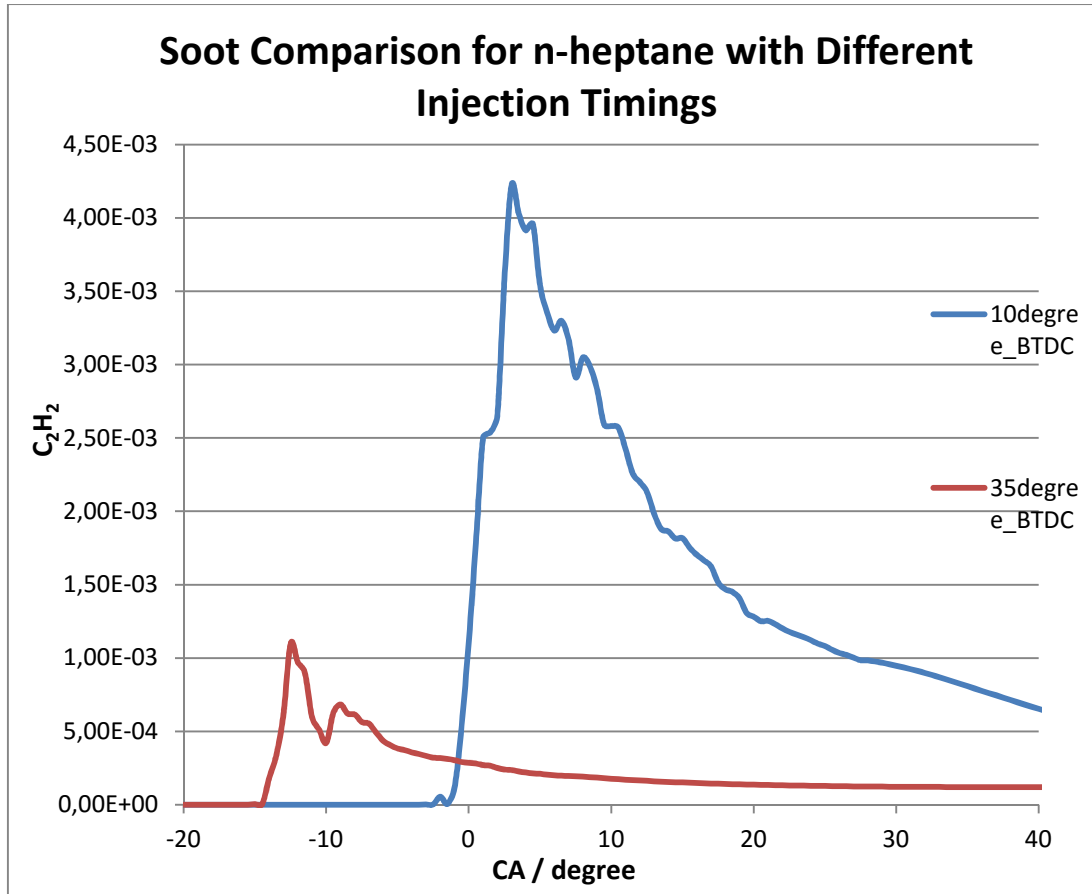


Figure 4.10 Soot comparison for different injection timings for n-heptane.

C₂H₂ (acetylene) is used as the soot inception species in the formation rate. The Figure 4.11 presents different injection timing effects on soot formation for n-heptane. As the injection timing is advanced, longer ignition delays lead to more fuel burning in the premixed phase. Therefore the soot emissions reduce (Choi, Choi, and Chung 2011).

Table 4.3 Properties of the fuels at standard atmospheric conditions.

Properties	Diesel	Heptane	Toluene	Isooctane
Density(kg/m ³)	827-840	680	867	692
Lower Heating value (MJ/kg)	42.5	44.8	40.6	44.3
Cetane Number	52	55	0	15
Boiling Point(°C)	169	98	111	99

In the table 4.3, it can be seen as volatility is higher than toluene. The addition of toluene should cause an increment in the soot particle mass concentrations, since the toluene is an aromatic compound and soot promoter. Therefore, toluene / n-heptane mixtures should have higher soot amount than long-chain hydrocarbon blends. However, toluene mixtures show lower soot in this study. Figure 4.12 and 4.13 show the results of C₂H₂ mass fractions.

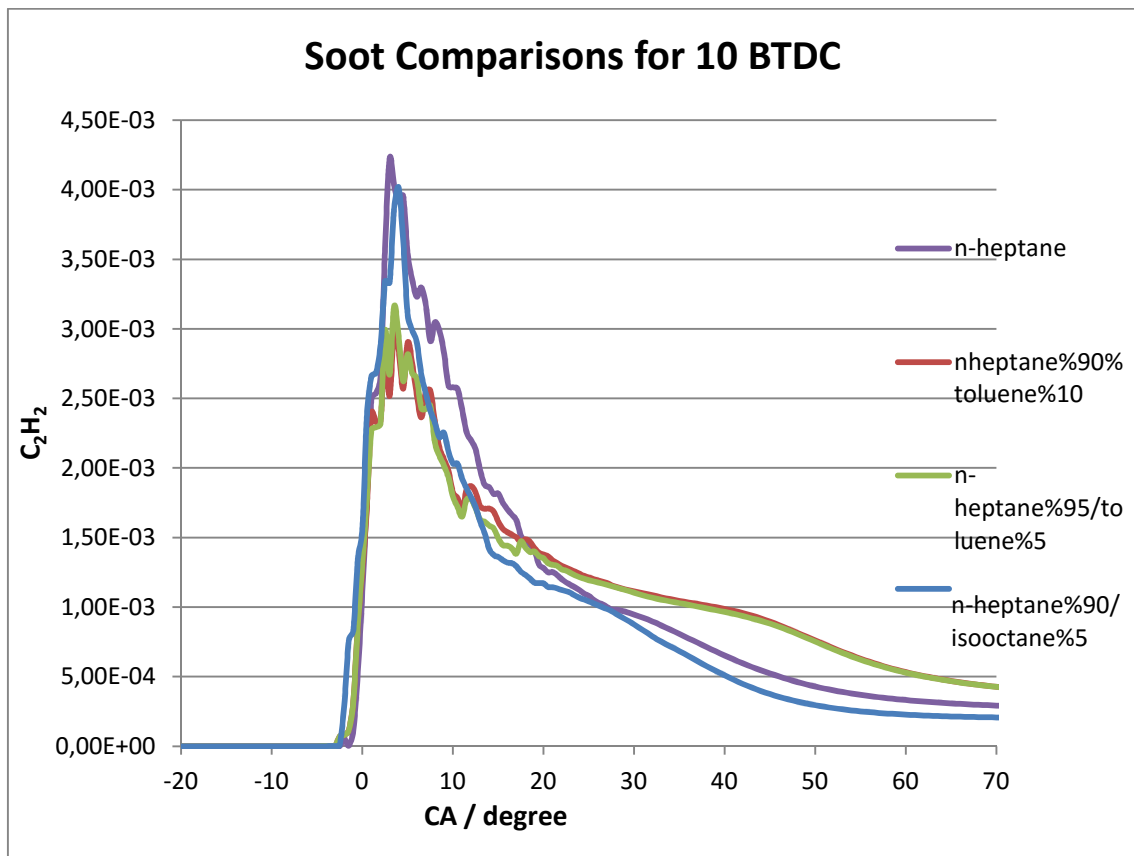


Figure 4.11 C₂H₂ results versus crank shaft for tested fuels (SOI 10° BTDC).

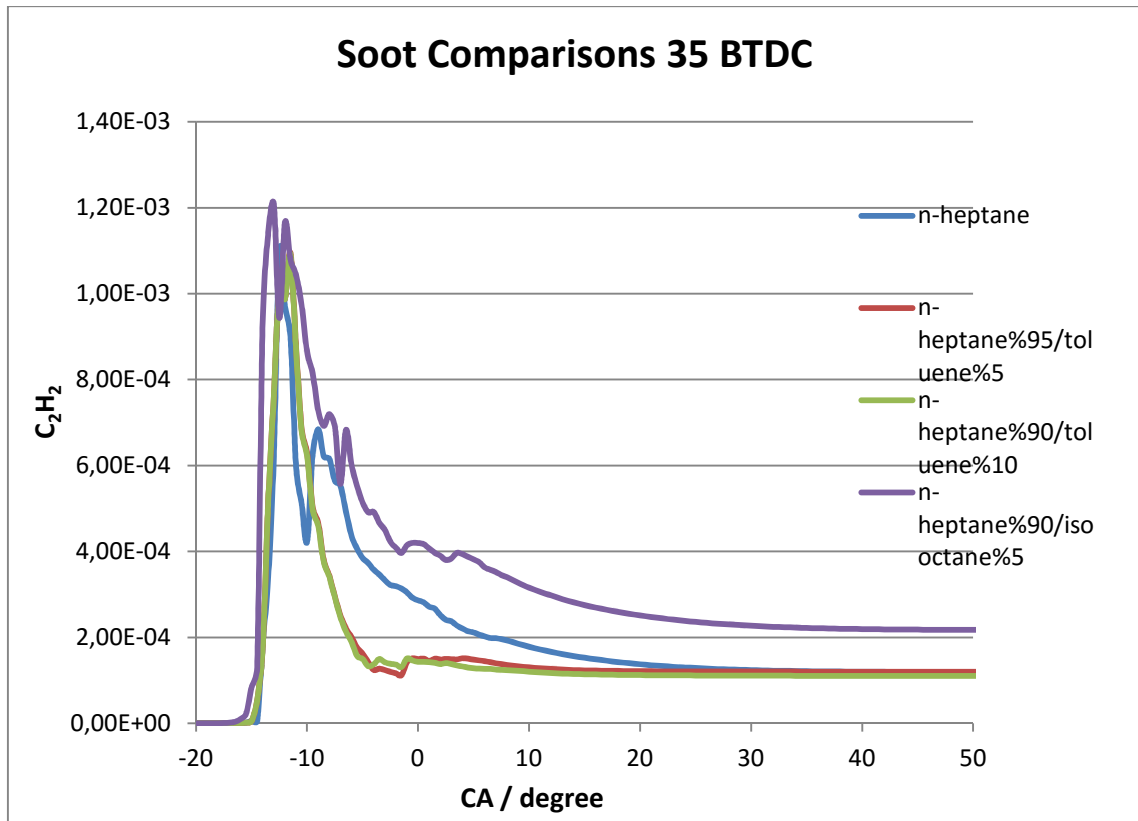


Figure 4.12 C_2H_2 results versus crank shaft for tested fuels (SOI 35° BTDC).

In reality, diesel engine fuels with low volatility and high cetane numbers inhibit the formation of a uniform mixture, hindering the fuel burning process. Also, the use of high viscosity fuels hinders vaporization, favoring the formation of large diameter droplets and causing incomplete combustion due to the high penetration of the fuel jet, hindering cold starts and increasing the emissions. The n-heptane and n-heptane / isooctane blend soot amounts were similar, since these molecules are straight-chain and isooctane boiling point is close to n-heptane ($99,5^\circ C$). The reason of the lower toluene soot amount is about the reaction path and reduced chemical mechanism (Ahmed, Mauss, and Zeuch 2009). Although, volatility of toluene was lower than n-heptane, there is no huge differences between boiling points of surrogate fuels. Same situation was considered for viscosities.

CHAPTER 5

CONCLUSION

Computational tools face enormous challenges because of the complexity of the fuel composition and the lack of the kinetic data in the combustion simulation of conventional hydrocarbon petroleum fuels. In order to provide solution to this problem, surrogate fuels, whose physical and chemical properties, and combustion characteristics are similar to the real fuel for combustion simulations, have been used in this study. This study presents numerical modeling for various surrogate fuels SRM.

The research goal for many numerical studies is to develop surrogate fuels that match experimental study results. However; physical and chemical properties of surrogate fuels are supposed to be matched with conventional diesel fuel properties to fulfil the the research goal. Many processes as ignition and soot formation, which are affected by the chemical and physical properties of the fuel, are dependent on both mixing and kinetically controlled processes. The results obtained from engine experiments (Diez, Løvås, and Crookes 2012), which include engine operating characteristics such as combustion phasing and duration, combustion efficiency, and primary emissions was considered the base data, and simulations were conducted according to these data.

The most important test to characterize fuel ignition quality is cetane number. In order to describe ignition quality, it has to include calculated cetane index, which is calculated from other fuel properties such as density and volatility, and derived cetane number calculated from the ignition delay. In this study, n-heptane, two n-heptane-toluene and n-heptane-isooctane mixtures were investigated with a computational tool called LOGEsoft. Surrogate fuels ignition delays and soot formations were examined. For the main component, n-heptane was choosen as straight chain hydrocarbon molecule, since it can be utilized easily to simulation tools.

The program was calculated ignition delay for the surrageate fuels which were compared to conventional diesel fuel experimental delay. When comparison was made, the ignition delays were found very similar to tested diesel fuel with respect to the

ignition delay. However, calculated ignition delays were slightly different than experimental diesel for n-heptane and n-heptane / toluene mixtures, differences between experimental and numerical studies are acceptable situation. The reason of the lower ignition delay for n-heptane / isooctane blend was probably occurred from isooctane structure. Since it was a paraffins and generally the activation energy to form free radicals and starting the oxidation process was low compared to that of isoparaffins and aromatic compounds. Besides, even under the conditions where the fuel/air distribution matches, the ignition behavior of n-heptane and real diesel can be different, because of the first stage (low temperature) heat release of n-heptane and real diesel will behave a different dependence on temperature and pressure. The reason of the differences can be the oxidation and pyrolysis kinetics of n-heptane. More specifically, the potentially strong effects on ignition of aromatics, cycloparaffins, and iso-paraffins are not described well by n-heptane kinetics.

Similar effects can be seen in soot formation. Even though after adding an aromatic component in to the mixture, soot behaviour was not the same with expectations. As a consequence, while engine experiments with n-heptane are qualified, they may not accurately reflect the combustion behavior of real diesel fuel. Similar limitations are expected to hold for any single component surrogate.

In order to have more accurate results more complex surrogate blends should be tested with LOGEsoft. In future studies, different aromatic compounds should be studied regarding volatility of the fuel and soot emission effects of the engine.

REFERENCES

- Ahmed, Ss, F Mauss, and T. Zeuch. 2009. "The Generation of a Compact N-Heptane/toluene Reaction Mechanism Using the Chemistry Guided Reduction (CGR) Technique." *Zeitschrift Für ...* 223 (4-5): 551–63. doi:10.1524/zpch.2009.6037.
- Aronsson, Ulf, Clement Chartier, Uwe Horn, Öivind Andersson, Bengt Johansson, and Rolf Egnell. 2008. "Heat Release Comparison Between Optical and All-Metal HSDI Diesel Engines" 2008 (724). doi:10.4271/2008-01-1062.
- Barkhudarov, M R, C W Hirt, D Milano, Flow Science, and General Comments. 2011. "C Ommments on a C Omparison of Cfd S Oftware for M Icrofluidic," 1–8.
- Bhave, Amit, Markus Kraft, Luca Montorsi, and Fabian Mauss. 2006. "Sources of CO Emissions in an HCCI Engine: A Numerical Analysis" 144: 634–37. doi:10.1016/j.combustflame.2005.10.015.
- Choi, B.C., S.K. Choi, and S.H. Chung. 2011. "Soot Formation Characteristics of Gasoline Surrogate Fuels in Counterflow Diffusion Flames." *Proceedings of the Combustion Institute* 33 (1). Elsevier Inc.: 609–16. doi:10.1016/j.proci.2010.06.067.
- Colban, Will F, Duksang Kim, Paul C Miles, Richard Opat, Roger Krieger, David Foster, Russell P Durrett, and Manuel a Gonzalez D. 2008. "A Detailed Comparison of Emissions and Combustion Performance Between Optical and Metal Single-Cylinder Diesel Engines at Low Temperature Combustion Conditions." *SAE Int. J. Fuels Lubr.* 1 (1): 505–19. doi:10.4271/2008-01-1066.
- Curl., R. L. 1963. "Dispersed Phase Mixing: I. Theory and Effects in Simple Reactors." *A. I. Ch. E. Journal*, 9(2):175– 181, 1–8.
- Curran, H J, E M Fisher, P Glaude, N M Marinov, W J Pitz, C K Westbrook, and D W Layton. 2001. "Detailed Chemical Kinetic Modeling of Diesel Combustion with Oxygenated Fuels." *Sae 2001-01-0653* 2001 (724).
- Çalık, Alper T, a Metin Ergeneman, and Valeri I Golovitchev. 2009. "Hesaplamalı Akışkanlar Dinamiği İle Dizel Motorlarında Emisyon Oluşumu ve Azaltılmasının Modellenmesi." *İTÜDERGİSİ/d* 8 (2): 93–104.
- Diez, Alvaro, Terese Løvås, and Rj Crookes. 2000. "An Experimental and Modelling Approach to the Determination of Auto-Ignition of Diesel Fuel, Dodecane and Hexadecane Sprays at High Pressure." *Uk.Cd-Adapco.Com*, 1–6.
- Diez, Alvaro, Rj Crookes and, and Terese Løvås. 2012. "Experimental Studies of Autoignition and Soot Formation of Diesel Surrogate Fuels." *Automobile Engineering*, 656–64. doi:10.1177/09544070124558402.

- Farrell, J T, N P Cernansky, and F L Dryer. 2007. "Development of an Experimental Database and Kinetic Models for Surrogate Diesel Fuels." *SAE Paper 2007*: 776–90. doi:10.4271/2007-01-0201.
- Kraft, Markus, Peter Maigaard, Fabian Mauss, Magnus Christensen, and Bengt Johansson. 2000. "Investigation of Combustion Emissions in a Homogeneous Charge Compression Injection Engine: Measurements and a New Computational Model." *Proceedings of the Combustion Institute* 28 (1): 1195–1201. doi:10.1016/S0082-0784(00)80330-6.
- Krishnasamy, A.a, R.D.a Reitz, W.b Willems, and E.c Kurtz. 2013. "Surrogate Diesel Fuel Models for Low Temperature Combustion." *SAE Technical Papers* 2. doi:10.4271/2013-01-1092.
- Liang, Long, Chitralkumar V. Naik, Karthik Puduppakkam, Cheng Wang, Abhijit Modak, Ellen Meeks, Hai-Wen Ge, Rolf Reitz, and Christopher Rutland. 2010. "Efficient Simulation of Diesel Engine Combustion Using Realistic Chemical Kinetics in CFD." doi:10.4271/2010-01-0178.
- Naik, Chitralkumar V, Karthik Puduppakkam, Cheng Wang, Jeyapandian Kottalam, Long Liang, Devin Hodgson, and Ellen Meeks. 2010. "Applying Detailed Kinetics to Realistic Engine Simulation: The Surrogate Blend Optimizer and Mechanism Reduction Strategies." *SAE Int. J. Engines* 3 (1): 241–59. doi:10.4271/2010-01-0541.
- Pepiot, Perrine. 2008. "Automatic Strategies to Model Transportation Fuel Surrogates," no. June. http://pepiot.mae.cornell.edu/pdf/Pepiot_Thesis.pdf.
- Pepiot-Desjardins, P., and H. Pitsch. 2008. "An Automatic Chemical Lumping Method for the Reduction of Large Chemical Kinetic Mechanisms." *Combustion Theory and Modelling* 12 (February 2012): 1089–1108. doi:10.1080/13647830802245177.
- Pitz, William J., and Charles J. Mueller. 2011. "Recent Progress in the Development of Diesel Surrogate Fuels." *Progress in Energy and Combustion Science* 37 (3). Elsevier Ltd: 330–50. doi:10.1016/j.pecs.2010.06.004.
- Przyby, Grzegorz, and Stefan Postrzednik. 2013. "THE HEAT TRANSFER COEFFICIENT CALCULATION IN THE ICE CYLINDER BASED ON IN-CYLINDER PRESSURE DATA" 20 (4).
- Puduppakkam, Karthik V, Karthik V Puduppakkam, Long Liang, Long Liang, Chitralkumar V Naik, Chitralkumar V Naik, Ellen Meeks, Ellen Meeks, Bruce G Bunting, and Bruce G Bunting. 2009. "Combustion and Emissions Modeling of a Gasoline HCCI Engine Using Model Fuels." *Library*. doi:10.4271/2009-01-0669.
- Saxena, Vivek, and Stephen B. Pope. 1999. "PDF Simulations of Turbulent Combustion Incorporating Detailed Chemistry." *Combustion and Flame* 117: 340–50. doi:10.1016/S0010-2180(98)00081-9.

- Seidel, L, F Bruhn, S S Ahmed, G Moréac, T Zeuch, and F Mauß. n.d. “The Comprehensive Modelling of N- Heptane / Iso-Octane Oxidation by a Skeletal Mechanism Using the Chemistry Guided Reduction Approach,” 1–5.
- Smallbone, A.J.a, N.b Morgan, A.a Bhave, M.b Kraft, R.F.c Cracknell, and G.c Kalghatgi. 2010. “Simulating Combustion of Practical Fuels and Blends for Modern Engine Applications Using Detailed Chemical Kinetics.” *SAE Technical Papers*. doi:2010-01-0572.
- Su, Xingyuan, Youngchul Ra, and Rolf Reitz. 2014. “A Surrogate Fuel Formulation Approach for Real Transportation Fuels with Application to Multi-Dimensional Engine Simulations.” *SAE International Journal of Fuels and Lubricants* 7 (1): 236–49. doi:10.4271/2014-01-1464.
- Tunér, Martin. 2011. “Studying the Potential Efficiency of Low Heat Rejection HCCI Engines with a Stochastic Reactor Model.” doi:10.4271/2009-24-0032.
- Yang, B. 1998. “An Investigation of the Accuracy of Manifold Methods and Splitting Schemes in the Computational Implementation of Combustion Chemistry” 32: 16–32.